A surface science approach to hydrogen storage

Ostenfeld, Christopher Worsøe; Chorkendorff, Ib; Dahl, Søren

Publication date:
2006

Document Version
Publisher's PDF, also known as Version of record

Ph.D. Thesis:

A Surface Science Approach to Hydrogen Storage

Advisor: Ib Chorkendorff, ICAT, Dept. of Physics. DTU

Christopher W. Ostenfeld

August 31, 2005

Preface

This thesis is submitted in partial fulfilment of the requirements for the Ph.D. degree from the Technical University of Denmark. The work has been carried out at the Department of Physics, within the Interdisciplinary Research Center for Catalysis(ICAT). Financial support was provided by the Danish Research Council, Center of Excellence, "Towards a Hydrogen-based Society". The advisors were Professor Ib Chorkendorff, Dept. of Physics, DTU, Senior Scientist Søren Dahl, Haldor Topsøe, and Senior Scientist Allan Schrøder Pedersen, from Risø National Laboratories.

I would like to gratefully acknowledge the insightful supervision from Professor Ib Chorkendorff, who, on a regularly basis, provided many ideas, and always showed tremendous interest in the project. I would also like to thank Jon Davies and Tejs Vegge for fruitful collaboration on one project. Martin Johansson is also to be thanked for helping with the modelling, and in general helping out around the lab. Also thanks to John Larsen for his invaluable assistance and general good spirit. Anders Andreasen is also acknowledged for helpful discussions.

I am deeply indebted to the craftmanship of Hans Christian Sørensen and Dan Shacham, who tirelessly provided essential equipment parts. Per Hellerup Jensen, Erik Hansen, and Poul Andersen are also acknowledged for helping out in various situations.

Thanks are extended to the entire crew at ICAT, for making my stay here pleasant and enjoyable.

Christopher Worsøe Ostenfeld

Kgs. Lyngby, 31. august, 2005

Abstract

The work here, entitled "A Surface Science Approach to Hydrogen Storage", concerns fundamental investigations of the magnesium-hydrogen interaction. The work is fueled by the quest to find alternative hydrogen storage materials, which is an essential part of a future hydrogen-based society. By studying well-defined magnesium films, unique insight can be gained into the atomic-scale processes occurring. By growing thin magnesium films, with thicknesses around 100 atomic layers, under ultra-high vacuum conditions, and subsequently dosing hydrogen we can model the workings of a functioning magnesium particle.

The first part of the work concerns the formation of ultra-thin magnesium films and the interaction with hydrogen. Here we find that hydrogen overlayers are adsorbed, and the findings are complemented by density functional theory calculations. We find, rather remarkably, that hydrogen cannot be released from magnesium, without magnesium sublimating.

The second part of the thesis concerns the interaction of magnesium with oxygen, a common impurity in magnesium-based storage systems. Here, it is found that magnesium sublimation can be heavily attenuated, as a result of surface oxidation. We suggest that the oxide impurities, always present in powders, actually constitute a necessity for cyclic stability in the powders to be obtained.

The last part concerns the interaction of well-defined magnesium films, with a high pressure of ultra-pure hydrogen, i.e. an exact replica of the conditions imposed on magnesium powders. Here, we find that the sticking probability of hydrogen on magnesium is extremely low, around $1{\cdot}10^{-13}$. Adding a platinum overlayer to the surface results in a drastic increase in

the sticking probability. However, the platinum overlayer is found to not be thermally stable.

Although, no novel magnesium-based alloys were found, we managed to suggest why cyclic stability can be achieved in powder systems. We also opened up the possibility of investigating hydrogen transport on magnesium oxide, as better comprehension of this could lead to increased understanding of the system.

Dansk Resumé

Denne afhandling, med titlen "En overflade-videnskabelig tilgang til brint-lagring", omhandler fundamentale undersøgelser af vekselvirkningen mellem magnesium og brint, studeret i et model system, under ultra-rene forhold, som kun kan opnås under ultra-højt vakuum. Arbejdet er inspireret af behovet for at finde et alternativt brint-lagrings medium, som er en vigtig brik imod overgangen til et brint-baseret samfund. Ved at studere vel-definerede magnesium film, opnår vi enestående indblik i de atomare processer. Ved at gro magnesium film, med en tykkelse omkring 100 atom-lag, under ultra-høje vakuum betingelser, og herefter dose brint, kan vi modellere det som foregår i en magnesium partikel.

Den første del omhandler dannelsen af ultra-tynde magnesium film, og disses vekselvirkning med brint. Vi finder at brint overlag adsorberes og er stabile, hvilket støttes af tætheds-funktional teori beregninger. Vi finder yderligere, i modsætning til ens intuition, at brinten først frigøres når magnesium opnår et væsentligt damptryk, hvilket ikke kan siges at harmonere med kravet om cyklisk stabilitet.

Den anden del handler om vekselvirkningen mellem magnesium og ilt, som er en almindelig urenhed i magnesium-baserede brint materialer. Her finder vi at magnesium fordampning kan hæmmes væsentligt, som følge af overflade oxidation. Vi foreslår at oxid urenheder, som typisk findes i pulverprøver, rent faktisk er en nødvendighed for cyklisk stabilitet i magnesium.

Den sidste del omfatter vekselvirkingen mellem vel-definerede magnesim film og et højt tryk af brint, med andre ord en eksakt simulering af det som foregår i et brint-lagrings system. Vi finder at spaltningssandsynligheden er meget lav, omkring 1 ud af 10000 milliarder brint molekyler spaltes ved 120

^{o}C. Ved at gro et overlag af platin på overfladen stiger sandsynligheden for spaltning.

Selvom der ikke, i løbet af dette projekt er dukket nye interessante legeringer frem, har vi fået en fornemmelse af hvorfor der kan haves cyklisk stabilitet i pulver prøver. Værket her åbner op for en dybere forståelse af vekselvirkingen mellem brint og magnesium oxid.

CONTENTS

CHAPTER 1

Introduction

The work presented here concerns the interaction of hydrogen with thin films, with the intent of studying hydrogen storage. In this chapter, the concept of a hydrogen-based society is briefly reviewed, along with some of the challenges which are faced in order for this transition to be realized. A short introduction into the field of hydrogen storage ensues, with a discussion of the different known (and not so known) containment methods.

1.1 Hydrogen-based society

Today, 3/4 of our energy consumption comes from burning fossil fuels, and our energy consumption today is 10 times higher than 100 years ago. At the current rate of consumption, oil and gas reserves will only last 40-60 years while coal reserves should take us into the 23rd century[1]. The prospect of a hydrogen-based society, based on renewable energy sources, is an attractive, almost utopic, scenario as it provides

the solution to a number of the problems which are at the forefront of todays society including global warming, oil prices, and inner city pollution. The economics of the future hydrogen society have been tabulated by, amongst others,Ogden[2], who argues that the economics of a society based on renewable energy can compete with current fuel prices, given certain technological breakthroughs.

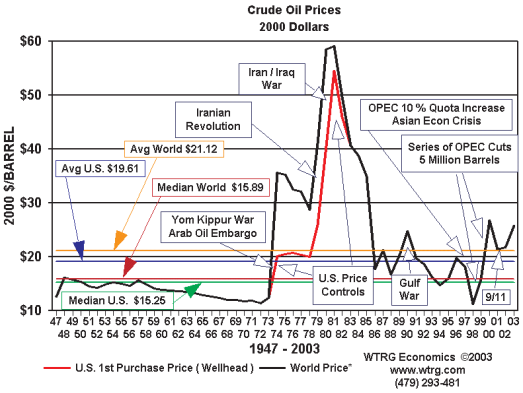

Figure 1.1: History of oil prices, from 1947 to 2003. From [3]

Figure 1.1 shows the oil prices over the past 50 years. We observe immediately several fluctuations in the price, due to various events in the Middle East, including the Arab oil embargo, Iran/Iraq War, and the Gulf War. The terrorist attacks on New York in 2001, also affected the price considerably, although the market rebounded fairly rapidly hereafter. The strong dependence of the oil price on the situation in the Middle East, raises the issue of energy security. By having an energy source which could be equally harvested by all countries, the current balance of power observed in the oil-producing nations will vanish. The fact that two-thirds of the oil available in the world is controlled by non-democratic nations also raises some concern.

1.1.1 Technological Challenges

The implementation of a hydrogen-based society will not only require political goodwill, possibly through heavier taxation of fossil-fuel based automobiles, and subsidising cars based on "clean" technology. In the United States, for instance, a 1500 USD tax break is offered to owners of gasoline-electric hybrid vehicles[4] The complete implementation will also require a number of technological breakthroughs in a number of fields, some of which are given below.

- Hydrogen Production: The cheapest way of producing hydrogen at the moment is from the steam reforming process, which is accompanied by CO_2 emissions, and a trace of CO is present in the hydrogen gas. Possible alternative routes to hydrogen production includes electrolysis, which benefits from the fact that no CO is present in the gas. Electrolytic production of hydrogen cannot, however, compete economically, with hydrogen produced by steam reforming, unless the

former is produced by cheap off-peak electricity[2]. Another possible hydrogen production route involves the photoelectrochemical materials, like TiO_2, whereby hydrogen can evolve from water, upon UV-illumination[5, 6].

- CO-resistant anode materials for low temperature proton-exchange membrane fuel cells: Due to CO traces in hydrogen feedstock, CO-resistance of the anode material is crucial. Current choice of anode materials include platinum and platinum-ruthenium alloys[7].

- Solid Oxide Fuel Cells(SOFC): SOFC's are based on an oxygen conducting membrane. The most common membrane is Yttria-stabilized ZrO_2. Various types of fuels are compatible with the SOFC. This type of fuel cell operates at high temperatures(typically above 850 °C), generating electricity. Heat is also evolved by the cell which can be used to run a turbine[8]. Since the SOFC runs at high temperatures, extreme demands are placed on the materials used, which necessitates high cost components. By reducing the operating temperature, cheaper materials can be used[9].

- Improved hydrogen storage materials: As will be mentioned in section 1.2 no material exists at the moment, which obeys the technical demands for mobile applications set forth by the U.S. Department of Energy, summarized in Table 1.1. For non-mobile applications, hydrogen storage in underground aquifers or salt caverns is also an option, for example, to store hydrogen created by electrolysis with off-peak wind power or electricity[10]

1.2 Hydrogen Storage

At the moment, 3 possible hydrogen storage options are available. Each is briefly described, with special reference to the current status of each technology.

1.2.1 High Pressure

High-pressure hydrogen gas containment remains the most popular storage method, with pressures around 200 bars being routinely used. Recent technological advances within the field of lightweight composite cylinders, allow for the pressure to be increased by a factor of 4. The main problem related to using conventional materials for high pressure hydrogen containment is

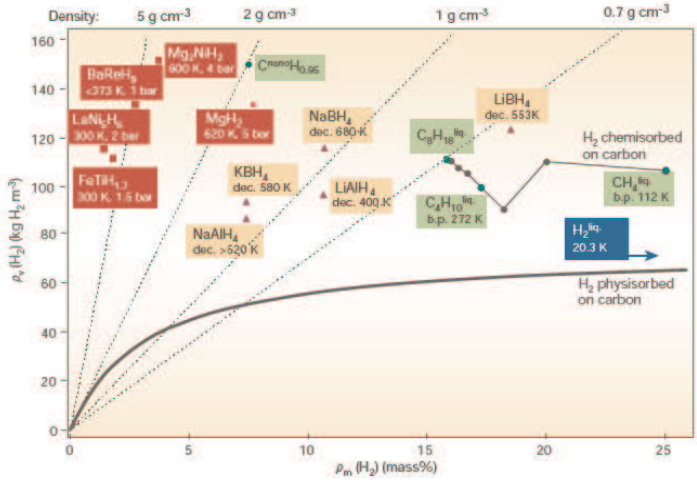

Figure 1.2: Comparison of different hydrogen storage options. From Ref.[14]

embrittlement, observed after numerous charging/decharging cycles[11]. The energy needed to compress the hydrogen is estimated at 18 % of the energy content. There are still some safety concerns, which suggest that consumer confidence in high pressure gas containment might present a problem.

1.2.2 Liquefaction

The technological expertise required to liquify hydrogen was developed during the early space age, as liquid hydrogen was brought along on the space vessels of the day to be used on the on-board fuel cells[12]. Due to the low critical temperature of hydrogen, liquid hydrogen vessels must be open, which results in boil-off losses. It is also possible to combine liquid hydrogen with a metal hydride, like Fe-Ti, and this way minimize hydrogen losses due to boil-off[13]. The energy costs associated with liquifying hydrogen are between 30-40 % of the energy content[12].

1.2.3 Metal hydride

Although the technological expertise behind both liquid storage and high pressure hydrogen containment is vast, there are, as mentioned above, certainly some practical problems, which cannot be circumvented, like safety concerns(for high pressure containment), and boil-off issues (for liquid storage). A third possibility presents itself, in the form of metal hydrides. The advantage of this method, is that the volumetric and cryogenic constraints are abandoned, by not having to store molecularly hydrogen directly, but

rather dissociating hydrogen and storing individual hydrogen atoms in a metallic lattice, through chemical bonding to a metallic host. In this way, hydrogen is stored in a safe and convenient way, in modestly priced materials. Figure 1.2 shows various hydrogen storage materials, along with the associated hydrogen release pressures and the temperatures necessary to achieve this pressure. Figure 1.2 does not contain information with the associated kinetics of hydrogen uptake and release.

1.2.4 Other

Apart from the 3 above-mentioned storage methods, carbon nanotubes have also been thought to present a possible storage alternative. Various groups have studied the material, and found incredible storage capacities[15, 16, 17], ranging from 7 to 67 wt%. While this, by far, was the most promising hydrogen storage material ever seen, there were certain reproducibility problems, and issues related to the effect of alkali dopants[18, 19]. Monte Carlo simulations suggest that carbon nanotubes will never adsorb more that around 1 wt% of hydrogen, rendering them unattractive in a hydrogen storage scenario[20]. Hydrolytic generation of hydrogen is also an option, but suffers from the drawback that on-board regeneration is not possible, requiring the entire storage module to be replaced, and regenerated centrally[21]. An example of hydrogen released via hydrolytic reaction is $MgH_2 + 2H_2O \rightarrow Mg(OH)_2 + 2H_2$, yielding a total storage capacity of 6.3 wt %.

1.3 Metal hydride systems

As discussed in the previous section, metal hydride seem to, in principle, offer a convenient way of storing hydrogen, by abandoning the view of hydrogen as an intact molecule. In other words

$$Me + H_2 \leftrightarrow MeH_2 + \Delta Q \tag{1.1}$$

One of the most attractive materials in the field is $LaNi_5$, reacts with hydrogen to form $LaNi_5H_{6.5}$. Unfortunately, only about 2 wt % of hydrogen is stored, but the hydrogen can be released at 2 bar, at ambient temperatures. The reason $LaNi_5$ releases hydrogen so readily, is that atomic hydrogen is bound in interstitial sites, obeying the so-called Westlake criterion. This states that hydrogen will be stable in lattice interstices provided a minimum hole size of 0.4 Å and a minimum H-H distance of 1.2 Å[22]. Another popular material is FeTi, which has a similar storage capacity, which is somewhat

compensated for by a fast response. As shown in Figure 1.2, higher storage capacity is achievable only by using light metals, like lithium, aluminium and magnesium, as host materials. Significant increases in the formation enthalpy of the hydride phase is accompanied with using light metals as storage materials. The formation enthalpy for $LaNi_5H_{6.5}$ is -30 kJ/mol and -28 kJ/mol for $FeTiH_{1.7}$, while it is -74.5 kJ/mol for MgH_2[23].

1.3.1 Complex hydrides

The use of alanates, or aluminohydrides, as hydrogen storage materials had historically been abandoned due to stability issues, related to the fact that the decomposition temperature of the material was somewhat above the melting temperature of the compound. However, in 1997 Bogdanovic and Schwikardi[24] made a critical breakthrough with sodium alanate, $NaAlH_4$, by using a titanium catalyst as well as Li-substitution, thus lowering both the decomposition temperature and the equilibrium pressure. At the present time, the exact role of the Ti doping remains somewhat unclear, and is currently the study of intense scrutiny in hydrogen storage materials circles[25, 26, 27, 28, 29] and is reviewed in Ref.[21]. The role of titanium has been thought to either be a hydrogen diffusion mediator or a hydrogen dissociation catalyst.

1.3.2 Mg-based hydrides

Magnesium hydride, MgH_2, can store up to 7.6 wt% of hydrogen, thereby rendering it attractive in the hydrogen storage. The hydrogen is bound very strongly, however, to magnesium, with an associated enthalpy of formation of -74.5 kJ/mol[23]. Although the list of potential hydrides, compiled in Figure 1.2, indicates that magnesium hydride is one of the most attractive hydrogen carriers, no information about the kinetics and thermodynamics of the hydriding process is included. In Chapter 2, this is covered in more detail.

1.3.3 Technical Goals

Table 1.1 lists the technical goals for a prospective hydrogen storage material, at different future stages. As we can see, very stringent demands are placed on the storage material and, at this point, no materials satisfy these demands. It is clear that the material must satisfy a number of goals, including low cost, cyclic stability, low delivery temperature, and delivery time.

Magnesium satisfies only the cost criterium and the 2010 storage criterium, and boasts a commodity trading price of 2 US$/kg[30][1].

Storage Parameter	2005	2010	2015
Usable specific Energy	4.5	6	9
Storage system cost($/kg H_2)	200	133	67
Cycle life(cycles)	500	1000	1000
Minimum Delivery Temperature(°C)	-20	-30	-30
Maximum Delivery Temperature(°C)	100	100	100
Minimum Delivery Pressure(atm)	2.5	2.5	2
Start time to full flow(at 20°C)(sec)	4	0.5	0.5
Refueling Rate(Kg H_2/min)	0.5	1.5	2

Table 1.1: U.S. Department of Energy Technical Goals for Hydrogen Storage. From Ref.[4].

1.4 Investigations of model systems

The goal of this project is to use a combination of conventional spectroscopic tools, used in surface science, including desorption-, electron- and scattering spectroscopy, in order to gain some insight into the fundamentals of magnesium-based hydrogen storage systems. As will be covered in subsequent chapters, the experimental facilities available allow for unique insight into the governing dynamics of the system. The advantage of using model systems in order to comprehend fundamental atomic-scale processes, is that a large degree of control can be exercised over the system, by defining a set of parameters, which can each be adjusted individually. The disadvantages associated with using a model system is that this approach is rather time-consuming, as strict demands are placed on sample cleanliness, and overall control of the system.

[1] Magnesium is usually produced by means of an electrolytic process, which means that the trading price is somewhat dependent on the price of electricity. For hydrogen storage applications, micron-sized magnesium particles would presumably become necessary, possibly produced through an atomization process, which would retail at a higher cost. Estimates of DKK 100/kg(1989), have been made by Vigeholm[31], dependent on the demand.

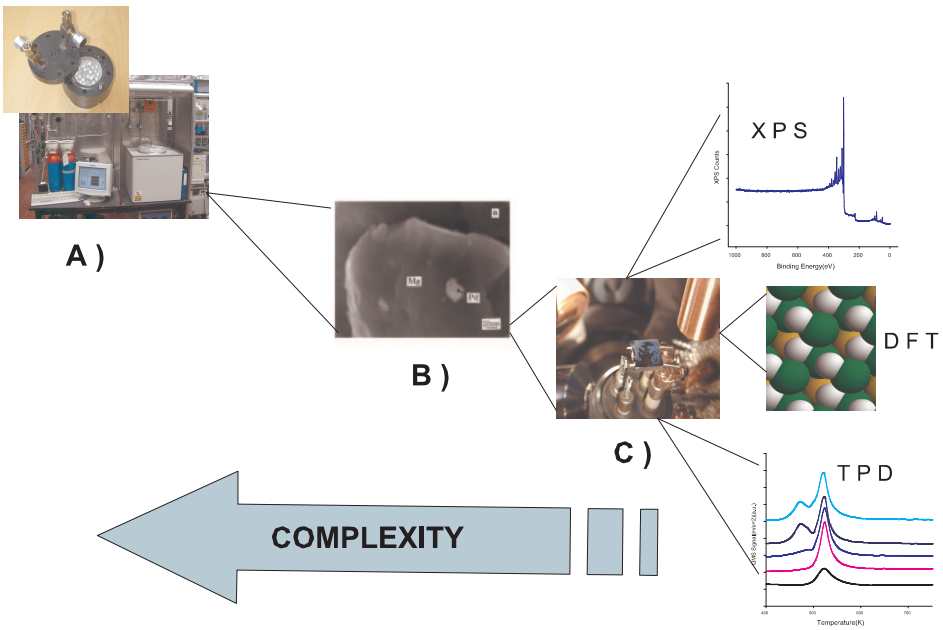

Figure 1.3: Schematic illustration, showing transition from state-of-the-art hydrogen storage system, to model system, as defined in this project. A) Hydrogen storage rig, capable of performing volumetric hydrogen uptake, on magnesium powder. B) TEM image of magnesium particle, with catalytic particle for hydrogen dissociation. From [32]. C) Experimental setup available in current project, allowing for combined surface analysis and high pressure hydrogen experiments.

1.4.1 Complexity Gap

Research into hydrogen storage are classically based upon mechanically treating powders, and, subsequently measuring isothermal sorption properties. The observable derived from this approach is an uptake rate, which corresponds to the sum of all events which comprise the sorption process, including dissociation, diffusion, and nucleation. As will be covered in later chapters, a substantial increase in complexity is accompanied with this process, due to the introduction of lattice stresses, and defects, during the milling process, thus complicating the analysis. Figure 1.3 shows the gap between a state-of-the-art hydrogen storage setup used for volumetric hydrogen uptake, Figure 1.3 A, and the laboratory equipment, which is to be used in this project, Figure 1.3 C.

The gap which has to be bridged in order for the model system approach to be valid, is that of complexity. In order for measurable hydrogen uptakes

to be measured on magnesium powders, in the setup shown in Figure 1.3 A, the powders are ball-milled, for various durations of time, usually for 10 to 100 hours[33]. The purpose of the ball-mill is to introduce defects, and to sever the protective oxide covering the particles. This means that, during hydrogen uptake experiments, the exact nature of the powders is not completely known. In the intended experiment, we will start with the simplest system, i.e. pure magnesium, and get a solid understanding of the simple system first. By, stepwise, increasing the complexity, adding catalysts and contaminants, we intend to bridge the complexity gap. As the experimental setup at our disposal allows for combined high pressure, and surface sensitive analysis, it allows for the possibility of a unique contribution to the field of hydrogen storage, as this approach has yet to be attempted.

CHAPTER 2

Magnesium

As magnesium is a promising hydrogen storage material, it has, correspondingly been studied in great detail. This chapter covers the theory of hydride formation, including a description of some model systems which involve magnesium. As will be discussed in this chapter the bulk of the work performed, has been on powder samples. However, some comprehensive studies on magnesium films have also been performed.

2.1 Hydride formation Theory

The formation of magnesium hydride can be reduced to the following sequence of events:

- Hydrogen transport from gas phase onto metal surface
- Molecular hydrogen diffuses to active site
- Hydrogen dissociation on surface
- Atomic hydrogen diffuses into the bulk. Formation of α-phase(solid solution of atomic hydrogen in magnesium
- Atomic hydrogen concentration increases, to the point where atomic hydrogen atoms start to mutually interact.
- Nucleation of hydride phase starts. β-phase(Metal hydride phase)

Figure 2.1, taken from [14], shows schematically the process. Figure 2.1 also shows correspondingly the **p**ressure-**c**omposition-iso**t**herm (PCT), relating the equilibrium pressure to the hydrogen uptake. At low hydrogen concentrations, the α-phase, i.e. the solid solution of hydrogen in magnesium, prevails. At increasing hydrogen concentrations, the atomic hydrogen in solid solution start to mutually interact, resulting in the onset of the nucleation of the β-phase, known as the hydride phase. This leads to a plateau of the pressure, at which the α and β phases coexist. At this pressure, which is temperature dependent, hydrogen can be extracted from the metal, simply by changing the pressure. All of this requires that the system is in equilibrium.

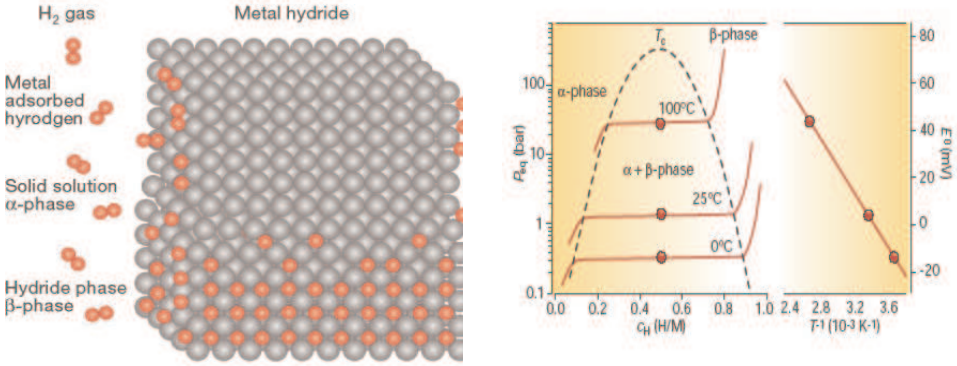

Figure 2.1: On left. Illustration, showing schematically the formation of a metal hydride, from molecular hydrogen. On right. Pressure-composition-isotherm. From [14].

By plotting the logarithm of the equilibrium pressure, as function of the temperature, the enthalpy of formation for hydride formation can be deduced, and is around -74.5 kJ/mol [23]. ΔS, which relates to the entropy change upon hydride formation is -135 J/(K mol). The enthalpy of formation and the entropy is related to the equilibrium as described in Equation 2.1.

$$ln\frac{p_{eq}}{p_0} = +\frac{\Delta H}{RT} - \frac{\Delta S}{R} \tag{2.1}$$

For magnesium, we find that at 600 K, the equilibrium pressure is 3.5 bars. Given that the above description is purely thermodynamical, a kinetic discussion must be introduced as well, especially since the use of metal hydrides as hydrogen storage materials places some critical demands on refueling(hydrogenation) and consumption(dehydrogenation), which were tabulated in Table 1.1 in Chapter 1.

2.2 Investigations of Magnesium

Magnesium is an extremely reactive material and reacts readily with oxygen, or residual water vapor. Although the oxidation process is self-limiting, typical oxide thicknesses are around 2 nm[34]. In order to use magnesium in a hydrogen storage framework, the surrounding oxide poses some problems, rendering magnesium powders seemingly useless, as prepared, due to the slow diffusion of hydrogen in magnesium oxide, at the temperatures where the material is usually used (between 300 and 400°C). Gonzalez and co-workers[35] found that hydrogen diffusion in MgO crystals could only be measured at temperatures above 1700 K. The activation process, as described by Chen and co-workers[36], is proposed to consist of a cracking of the oxide film, thus exposing metallic magnesium areas, which are more receptive towards hydrogen. The cracking process proceeds only when the sample is heated to 400 °C.

2.2.1 Hydrogen activation and diffusion

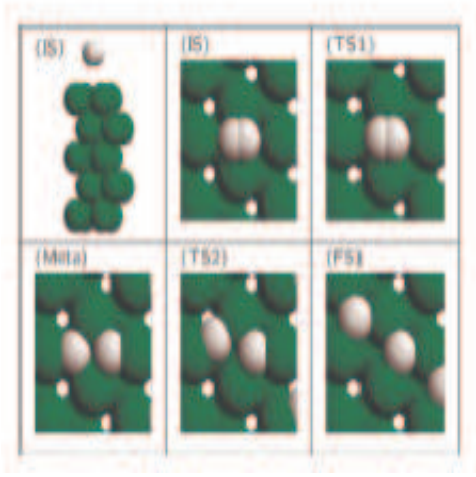

Figure 2.2: Dissociation pathway for a hydrogen molecule on the Mg(0001) surface. From [39]

First-principles investigations of the dissociation of hydrogen on magnesium yield values for the activation barriers. Bird and co-workers[37] have studied the system, using a local-density functional theory approach. Here, a barrier of 0.37 eV/molecule is found, with dissociation occurring over a bridge site, which is found to be higly favored over the top site.

A chemisorbed molecular state is found to be absent. Nørskov and co-workers[38], using a jellium approach, within the local-density approximation, find, a barrier of 0.5 eV, but unlike [37], a chemisorbed molecularly state is found to exist. Dissociation is also found to take place on a bridge site. Vegge[39] finds a much larger barrier for dissociation, just above 1 eV, using density functional theory. Vegge[39] also concurs that dissociation takes place at a bridge site, and finds no chemisorbed molecular state exists. The dissociation pathway for hydrogen dissociation, as suggested in [39], is shown in Figure 2.2. The diffusional properties of atomic hydrogen in atomic magnesium have also been investigated by Vegge[39] and Jacobson[40].

The diffusional properties of hydrogen in magnesium have been measured by, Nishimura and co-workers[41] and Renner and Grabke[42], who find activation barriers for hydrogen between 24 kJ/mol and 40 kJ/mol[1] The overall diffusion coefficient for the complete transition from magnesium to magnesium hydride has been measured by Spatz and co-workers[43], and was found to be $1.1{\cdot}10^{-20}\mathrm{m}^2/s$. If we try, on the basis of this diffusion constant to calculate the time necessary to form a hydride, using the equation $< x >_{1/2} = \sqrt{2Dt}$, we see that diffusion will limit the process even for 100 nm particles[2].

2.2.2 Mechanical Alloying/Ball-milling/Reactive-milling

Hydrogen uptake in magnesium powders has conventionally been performed by volumetric measurements, which allows the hydrogen flowing into a powder sample to be measured by means of mass flow controllers, at different pressures and temperatures. **P**ressure **c**omposition iso**t**erms(PCT), shown in Figure 2.1 are obtained in this manner[44]. Simple uptake curves, as function of time, at constant pressure and temperature can also be found. Uptake curves measure the sum of the individual events involved in hydride formation, given in Section 2.1. By fitting the uptake curve, one can obtain activation energies for absorption and desorption of hydrogen[45, 46]. By using this approach, Andreasen and co-workers[47] have compiled large discrepancies in the absorption/desorption energies for hydride formation/decomposition, and argue that sample preparation, and in particular the presence of oxide contaminants, results in a larger apparent activation energy.

Apart from using a volumetric type approach to monitor hydrogen up-

[1] In [42], the diffusion measurements are made on a Mg-Ce alloy, which could explain the difference, as pointed out in [41].

[2] Completely hydriding a 100 nm particle would require 126 hours, according to this overall diffusion coefficient.

take, the candidate materials are usually ball-milled, with the intent of reducing crystallite size, introduce defects and prepare Mg-based alloys. Magnesium has a low melting point and a high vapour pressure, which means that traditional metallurgical methods cannot be applied when trying to form novel magnesium-based materials. An unfortunate consequence of using the ball-mill approach is that by subjecting the material to this rather extreme preparation method, most chemical information is lost.

A general point which unifies most work concerning ball-milled powder samples is that sample characterization is carried out by means of XRD and TEM-EDX, which lack the ability to spot oxide impurites. Also, sample handling often includes exposure to air. The hydrogen sorption properties of magnesium are extremely sensitive to impurities, which makes a general comparison of different samples, obtained from different scientific groups difficult. Zaluska and co-workers[32] have carried out a systematic study of the effect of particle size, morphology and different additives, which is coherent. Figure 2.3 shows, for instance, the obvious effect of adding a small amount of platinum-group metal, like palladium, to the surface of magnesium. The authors also argue that when the grain size is reduced, the microstructure is changed, leading to an multitude of defects and grain boundaries, on which hydride nucleation can proceed more easily. The authors also studied the addition of a number of different additives, like lithium, aluminium, titanium, vanadium, manganese, zirconium and yttrium, and mixtures thereof. In general, the positive effects of the additives are presumed to be of a catalytic nature, while, in one case, a new alloy, consisting of magnesium, yttrium and zinc, is formed which has novel thermodynamic properties. Gutfleisch and co-workers found, that adding a PGM[3] to magnesium had no effect of desorption of hydrogen, due to diffusion into the bulk[48]. However, different milling times were employed in [32] and [48], making a direct comparison difficult. However, immobilisation of a hydrogen dissociation catalyst, is a prerequisite. Catalyst immobilization is suggested by [32], through TEM investigations, before and after hydrogenation.

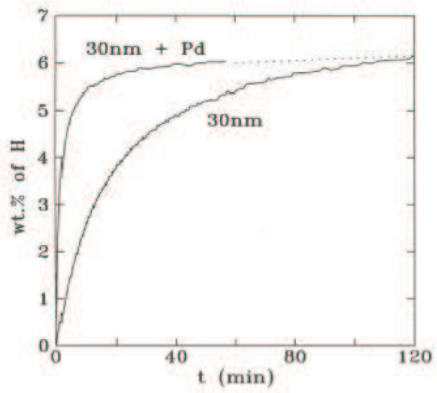

Figure 2.3: Effect of Pd catalyst on hydrogen uptake. T= 573 K, and P(H_2)= 10 bar.) From [32]

[3]Platinum Group Metals(PGM) cover the following 6 metals. Platinum, Palladium, Rhodium, Ruthenium, Iridium, and Osmium

A last possibility, which is used for studying hydrogen interaction with interesting storage candidates, involves reactive milling, whereby the metal of choice is ball-milled in a hydrogen atmosphere, where the continuous formation of fresh metal durfaces facilitates hydride formation[49]. Information about hydrogen desorption can be obtained by means of calorimetric investigations.

2.2.3 Thin film-based

A model system which has been popular in the field of magnesium-based hydrogen storage is the palladium-covered magnesium film. The system will be described, as well as some of the knowledge which has been extracted from several investigation, as the thin-film approach comes to closest to the intended approach of this project. By adding palladium to the surface, the barrier for hydrogen dissociation is essentially eliminated.

Krozer and Kasemo[50] initially studied the Pd/Mg system and learned that, at room temperature, stoichiometric MgH_2 was not formed, and that there was an inverse dependence of the saturation uptake on the hydrogen pressure. This was measured with the help of a quartz crystal microbalance. The inverse dependence was ascribed to the formation of a hydride at the interface between the palladium(62 Å) and magnesium film(7800 Å), and was offered as a possible explanation to the slow kinetics of hydrogenation of magnesium observed. Hjort and co-workers[51] studied the same system (Pd(70Å) and Mg(3800Å)), at 350 K, through resistivity measurements. This method works, due to the metal-to-insulator transition experienced upon hydride formation. As pointed out by Krozer and Kasemo[52], extreme alloying in the Pd-Mg system is observed at temperatures above 375 K. Alloying is verified by depositing a 10-20 nm palladium film on top of a magnesium film, and performing Auger Spectroscopy at various temperatures. At 412 K, a magnesium signal is seen through the film, due to alloying. Due to the probing depth of Auger spectroscopy, it is not possible to study the Pd/Mg interface directly, and alloying/intermixing therein. Yoshimura and co-workers[53] have also stud-

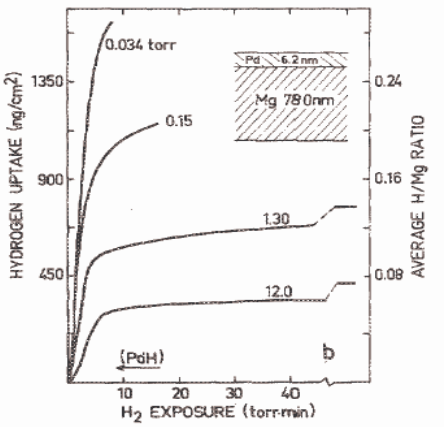

Figure 2.4: Hydrogen uptake, as measured through incremental mass increase, as measured by a quartz crystal microbalance. From [50]

ied the system and found intermixing at the palladium-magnesium interface even at room temperature. This was confirmed by sputter profiling. They find, furthermore, that the hydrogen is completely absorbed within the space of 5 seconds, at room temperature[4]. Other recent findings involve the work of Higuchi and co-workers[54, 55] who also studied the Pd-Mg system. Two main points were discussed in the 2 papers mentioned.

- Hydrogen was found to desorb at lower temperatures, around 400 K, for less-ordered Mg films
- Hydrogen was found to desorb at lower temperatures, around 360 K, for Mg films subjected to strain.

Due to the preparation technique, and particularly the hydriding conditions[5], it cannot be ruled out that some Pd-Mg alloying in fact occurs. If this is the case, it is not entirely certain if the observed desorption temperatures are, in fact, an artifact of this. Furthermore, cyclic stability of the material is highly questionable[6] due to the reasons mentioned above. Experimental investigations aimed at understanding the interaction between a well-defined magnesium surface have been performed by Sprunger and Plummer[56], where a meta-stable hydride phase was formed, upon hydriding a Mg(0001) surface with an atomic hydrogen source.

2.3 Unresolved issues

While there exists general consensus that micro-engineering magnesium into nano-grains or nanoparticles, has beneficial effects on the overall sorption rates, and adding a catalyst to the surface improves sorption kinetics, an overall experimental description of the sorption process is lacking. Amongst other things, the following questions can be raised.

- Is interfacial hydride a consequence of Pd/Mg interface, and if so is Pd/Mg a relevant system to study.
- What is the role of oxygen?
- What is the barrier for hydrogen dissociation on Mg? Can it even be measured. Is the barrier for hydrogen activation on a MgO-Mg ensemble lower/higher than on Mg.

[4] Subsequent sputter profiling experiment clearly indicate that the extent of hydrogenation is closely related to the extent of oxide impurity in the magnesium film.

[5] 0.1 MPa for 24 hours at 373 K

[6] The authors heat the system up to 700 K, and recharge the film with hydrogen.

- What is the mobility of the catalyst during hydrogenation/dehydrogenation?
- Why is there any cyclic stability of magnesium, when the material evaporates at alarming rates at the temperatures where magnesium hydride has been seen to work as a storage material for H_2. The vapor pressure of magnesium at 600 K, is $2{\cdot}10^{-4}$ torr.

These issues will be addressed in the forthcoming chapters.

CHAPTER 3

Experimental Methods

As mentioned in the Chapter 2, the vast majority of experimental work detailing the hydrogen-metal interaction for the case of magnesium is based on ball-milling studies, and corresponding volumetric measurements. In this work, we try to impose the same hydrogen conditions, i.e. high pressure, and elevated temperatures, on well-defined Mg thin films. By using a standard surface science approach, it was the hope that the hydrogen-metal interaction could be mapped out in some detail, and hopefully contribute to the understanding and improvement of Mg-based hydrogen storage materials. In this chapter, the experimental methods used are described, with special reference to their applicability in the investigation of hydrogen storage in magnesium.

3.1 Experimental Setup

The experimental setup used is basically the same as the one described in Ref.[57], but is briefly introduced here. Along with standard surface science tools, which are described in Section 3.2, the chamber is equipped with a high pressure cell, which allows hydrogen exposures of magnesium films, at pressures up to 4 bars, without seriously destroying the vacuum in the rest of the chamber. The typical pressure increase observed in the main chamber was of the order 10^{-6}-10^{-7} mbar at the highest HPC pressures. The sample is isolated from the rest of the chamber, through the use of a pair of knife-edges, which are depressed on either side of a OFHC[1] gasket. The single

[1] OFHC: **O**xygen-**f**ree **H**igh **C**onductivity Copper

crystal was mounted on W wires, with diameters between 0.4 and 0.5 mm. The thermocouple used was type K, and was spot-welded onto the crystal. The sample could be cooled to 135 K, by passing liquid nitrogen directly into the copper feedthroughs. Additional pumping of residual background gases was achieved through the use of a titanium sublimation pump(TSP), which could also be cooled with liquid nitrogen, for increased pumping speed[58]. The chamber is pumped by an Edwards diffusion pump, which can be separated from the chamber by means of a viton sealed valve. A liquid nitrogen trap is situated above the diffusion pump. 2 auxiliary turbomolecular pumps from Pfeiffer Vacuum are also present: One pumps the gas manifold while the other one pumps the high pressure cell, as well as differential pumping of the mass spectrometer(Balzers) and the ion gun (Perkin Elmer). The setup is furthermore equipped with a dual X-ray source and bipolar hemispherical analyzer, both from VSW. A base pressure below $1{\cdot}10^{-10}$ mbar was routinely obtained, in the chamber, following bake-out.

3.2 Applied Techniques

This section describes briefly the main experimental methods used in the project.

3.2.1 X-ray induced Photoelectron Spectroscopy

X-ray induced photoelectron spectroscopy, is an analysis method based on irradiating a conducting sample with soft monochromatic x-rays, and subsequently analysing the energy of the electrons which are emitted from the sample. The kinetic energy of the emitted photoelectrons is related to the binding energy (E_{bin}), the energy of the excitation source ($h\nu$), and the work function (ϕ_s) in the following manner:

$$E_{kin} = h\nu - E_{bin} - \phi_s \tag{3.1}$$

The equipment used offers the choice of both the Al Kα line(1486.6 eV) and Mg Kα line(1253.6 eV). A consequence of using low energy X-rays, is that the emitted electrons which are measured are only coming from the outer atomic layers of the sample, inspite of the fact that the X-rays are penetrating deep (order of μm) into the sample. As pointed out by Spatz and co-workers[43], XPS is very effective at tracking the metal to metal-hydride transition, in magnesium, due to the clear chemical shift associated with this transition, see Figure 3.1. However, due to the complication that MgH_2 is an insulator, care must be exercised when interpreting XPS spectra, due

to charging effects. Chemical shifts for the formation of magnesium hydride have been reported to be between 1.9[59] and 2.3 eV[43].

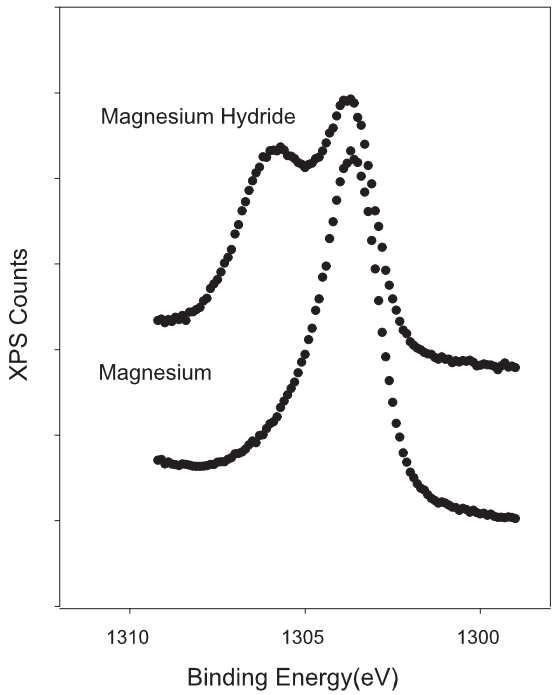

Figure 3.1: XPS spectra of the Mg 1s line, for magnesium hydride and metallic magnesium. hν=1486.6 eV.

3.2.2 Ion scattering Spectroscopy

Ion scattering spectroscopy, is a surface sensitive technique whereby light noble gas ions, like helium, are directed into the surface, at a constant kinetic energy. The vast majority of the ions will be neutralized. The kinetic energy of the scattered ions which have not been neutralized, is recorded in an electrostatic analyzer. The kinetic energy of the scattered ion is related to the mass of the atom where the helium ion was scattered, in the following relation:

$$\frac{E_1}{E_0} = [\frac{\sqrt{M_s^2 - M_i \sin^2\theta} + M_i \cos\theta}{M_s + M_i}]^2 \tag{3.2}$$

where M_s is the mass of the scatterer, M_i is the mass of the helium ion, and θ is the angle between the analyzer and the ion gun. By performing uptakes as function of metal deposition, the method allows us to study surface phenom-

ena such as surface segregation[60] and metal-on-metal growth[61]. Figure 3.2 shows the growth of magnesium on molybdenum. Due to the low mass of magnesium, ion scattering proved to be very invasive, due to sputtering of the overlayer. By reducing the ion flux, increasing the analyzer aperture, and decreasing the measuring time, we were able to completely eliminate magnesium sputtering.

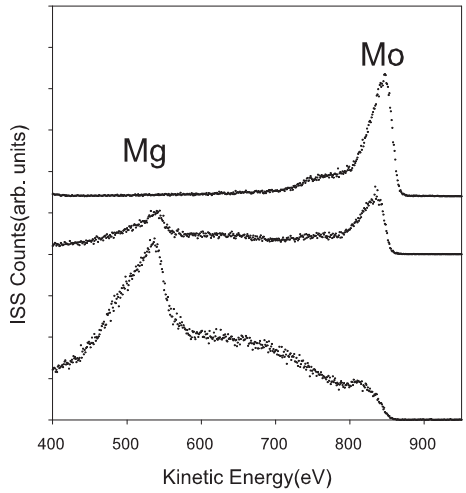

Figure 3.2: Ion scattering spectra(He^+), mapping out Mg on Mo growth. E_{kin}= 1000 eV.

3.2.3 Temperature Programmed Desorption

By heating the sample at a constant rate, typically 3 K/s, in front of a differentially pumped mass spectrometer, we can monitor ion currents corresponding to different mass:charge ratios desorbing from the surface. By, furthermore, assuming that no readsorption occurs, we can make quantitative assumptions regarding desorption kinetics. In the present work, we monitor the simultaneous desorption of metal(magnesium) and hydrogen. As the ion current resulting from metal detection in the mass spectrometer is 3 orders of magnitude less than for a gas, long measuring times, and high SEM settings were necessary in order to extract the details of metal desorption. Typical desorption spectra are shown in Figure 3.3.

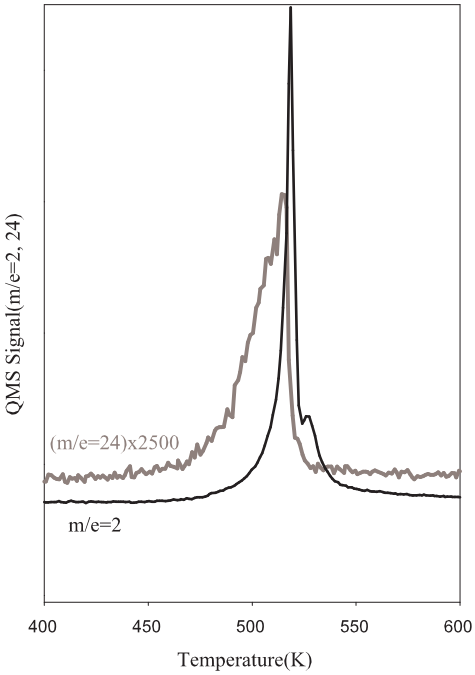

Figure 3.3: Simultaneous thermal desorption of magnesium and hydrogen, from a magnesium hydride film formed by means of an atomic hydrogen doser. The magnesium signal has been appropriately scaled. This is covered in some detail in Chapter 4

3.2.4 Quartz Crystal Microbalance(QCM)

A commercial quartz crystal microbalance operating at 6MHz, from Maxtek, was used in order to monitor evaporation rates. In short, the QCM works by oscillating at a characteristic frequency. The frequency changes when the crystal becomes loaded with material, e.g. metal from an evaporator source. By knowing the material density, the evaporated mass (usually ng/cm^2) can be converted to a thickness, in units of Ångstroms. An alternative use of the QCM involves real-time tracking of chemical reactions, i.e. metal oxidation[62] and hydride formation[51].

3.2.5 Choice of substrate

As we are interested in measuring the intrinsic hydrogenation properties of magnesium, the substrate onto which the films are evaporated must not alloy with the hydrogen storage material. Previous work, based on mag-

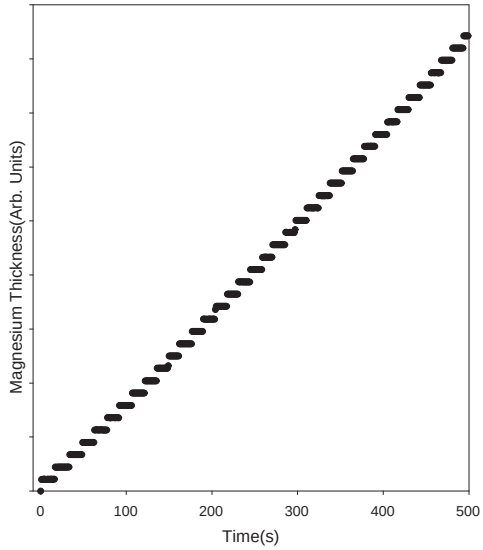

Figure 3.4: Mg evaporation rate, as registered by the quartz crystal microbalance, indicating temporal stability.

nesium, is mostly based on using palladium as a substrate which, at the same time, doubles as a source of hydrogen. This was covered in Chapter 2. When perusing the available literature concerning well-defined magnesium films deposited on single-crystal substrates[63, 64, 65], it becomes clear that popular substrates are molybdenum and ruthenium. As such, Mo(111) was chosen as a substrate. In the literature, molybdenum is acknowledged as being relatively difficult to clean. The most commonly used cleaning procedure consists of cycles of oxidation at 1273 K, followed by a flash to 2000 K. The first step is to remove carbon impurities, and the second step is to evaporate molybdenum oxide. We realized that heating to 2000 K was not possible, with the available setup, which is why we settled on sputtering at 1073-1273 K. It was, however, difficult to completely remove oxygen from the surface. By evaporating magnesium onto the surface, MgO_x was formed which could be sputtered away, or flashed off at 1500 K[64].

3.2.6 Metal Vapor Deposition

This section briefly covers the evaporation of metals used in this work.

Magnesium evaporator

A reliable evaporator had to be designed, with the intent of reproducibly providing set thicknesses of magnesium. As thick films were being deposited, it was important that the evaporator was stable, during the course of evaporation. After trying and abandoning several designs, we settled on a modified e-beam evaporator, operating without a bias voltage. The W filament had a diameter of 0.5 mm. The magnesium source, was placed in a molybdenum crucible, in the form of high purity(99.99% Goodfellow) magnesium rods, with lengths of approximately 3-5 mm. The metal source was heated by means of relatively gentle radiative heating from the filament, looped around the crucible. The evaporator was able to produce evaporation rates ranging from 0.02 to 0.4 Å Mg per second, at powers between 40-60 W. Prior to use, the evaporator had to be activated for 30-60 minutes, at high power, i.e. 60 W-70 W, in order to crack the oxide shell covering the magnesium rods. The onset of evaporation was registered by using the quartz crystal microbalance. The evaporator was able to reproducibly evaporate high purity magnesium films, as detected by XPS and ISS.

Platinum evaporator

Platinum was evaporated by tightly wrapping Pt wire(0.125 mm) around a W filament(0.25 mm), through which current is passed. At a power of around 30 W, a deposition rate around 0.1 Å/minute was obtained. The evaporator could be cooled with water in order to prevent out-gassing. Higher deposition rates were not possible, due to the complication that platinum began to alloy with the tungsten filament at increasing power, thus destroying the filament. Characterization of surface overlayers revealed that no tungsten had been deposited at the deposition rates used.

CHAPTER 4

H_2/Mg/Mo(111)

To gain insight into the fundamentals of the hydrogen-magnesium interaction, an experiment was designed which, on the one hand elucidated and complemented some previous work performed by Sprunger and Plummer[56], who had studied the fundamentals of the magnesium-hydrogen interaction, and on the other hand accurately described the study of hydrogen overlayers, at increasing magnesium coverages, deposited on a hydrogen-loaded substrate.

4.1 Introduction

The purpose of this work, was to study the magnesium-hydrogen interaction on a Mo(111) single crystal. Due to collaboration with a theorist performing density functional calculations, it became possible to describe a simple epitaxial system, which, on the one hand, suggested a possible structure for the magnesium overlayer, and, on the other hand, predicted a stable hydrogen state, which was formed as a consequence of the geometrical arrangement of the magnesium overlayer, as well as coupling to the metallic substrate.

4.2 Experimental background

Magnesium, being a simple metal, does not dissociate hydrogen, at UHV-compatible pressures. For a discussion of the relevant barriers for hydrogen dissociation, see p. 13. Initial experiments were performed, where a magnesium film was subjected to a $1{\cdot}10^{-4}$ mbar for 300 s, at 343 K, confirmed this.

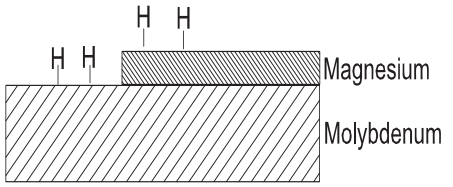

Figure 4.1: Schematic illustration of underlying principles of Chapter 4

The idea behind the experiment, was that the molybdenum substrate would easily dissociate hydrogen. By furthermore decreasing the temperature, we would be able to increase the hydrogen coverage during Mg deposition, if magnesium was deposited in a hydrogen backpressure of $2{\cdot}10^{-6}$mbar. It was clear that once the Mg film covered the Mo substrate, no more hydrogen would dissociate, and hence the molybdenum substrate served as a limited source of hydrogen to the growing Mg overlayer. A schematic representation of the situation is shown in Figure 4.1.

4.2.1 Experimental Details

To minimize background adsorption of residual gases such as CO and water in the chamber during hydrogen adsorption experiments, the manipulator was cooled with liquid nitrogen during experiments. This resulted in swift cooling rates and enhanced cryo pumping. All filaments, except the evaporator, were, furthermore, switched off during magnesium deposition to eliminate hydrogen cracking elsewhere but the surface. The extent of hydrogenation is monitored through combined use of TPD and XPS. The most surface-sensitive line, i.e. Mg 1s, was chosen as the XPS line of choice. This required the use of the Al Kα line, with a photon energy of 1486.6 eV. All TPD spectra were recorded at a linear rate of 3 K/s, using a Balzers quadrupole mass spectrometer. A SEM voltage of 2500 V was necessary in order to accurately map out the magnesium desorption, due to the low detection cross-section of the metal. The quadrupole mass spectrometer is enclosed in a copper housing, with a 3 mm aperture at the end. This way, we can minimize signal contributions from other surfaces in the chamber, including the crystal edges and heating wires and concentrate on the center of the crystal. Surface cleanliness was monitored with both XPS and LEISS. No indication of surface contamination of the Mo(111) crystal or the evaporated magnesium films was observed by XPS or LEISS. The hydrogen quality used was N57 which was subsequently passed over a reduced Cu catalyst and a molecular sieve. Hydrogen pre-dissociation was performed by passing the gas over a hot tungsten filament, operated at 40 W. The hydrogen doser was water-cooled to minimize outgassing during the dose. The amount of hydrogen desorbing from the surface, and thereby the hydrogen loading in the Mg film, can be calibrated on the basis of saturating the Mo(111) surface with hydrogen, forming a Mo(111)-3H structure[66], and normalizing all other hydrogen TPD spectra with respect to this TPD spectrum. As the crystal

could only be cooled to 135 K (compared to 80 K in [66]), a minor error can be expected in the absolute hydrogen coverages. However, based on the observed desorption profile, and comparing with work done by Fukui et. al [67] , we believe that the error incurred by this is minor. The experimental work is supplemented by theoretical calculations using density-functional calculations.

All hydrogen and magnesium coverages in this chapter are normalized with respect to the Mo(111) unit cell, i.e. a surface density of $5.86{\cdot}10^{18}\frac{1}{m^2}$.

4.3 Results and Discussion

4.3.1 Mg Epitaxy

The growth of magnesium on transition metal substrates has been studied in detail by several groups. Huang and co-workers, for example[65], have studied magnesium on Ru(001), and assigned monolayer desorption, on the basis of separate peaks in the magnesium desorption profile. Gallagher and co-workers[68], have studied magnesium growth on close-packed molybdenum, and found, using LEED and STM, unusual structural relaxation in the metal overlayer, for thicknesses above 4 ML. In this work, we combine low energy ion scattering, with TPD, and DFT, in order to suggest a structure of the overlayer.

Figure 4.2 shows magnesium TPD spectra, for increasing coverages. At low coverages, a single high temperature peak is seen. As the coverage is increased further, a new peak occurs, at 675 K, and finally, a sharp peak is seen at 500 K. The three peaks are interpreted as the first, second and third monolayers, respectively, growing epitaxially on the open Mo(111) surface. On the basis of the low temperature desorption peak, we calculate the heat of sublimation to be 138 kJ/mol, in agreement with similar investigations by Wu and co-workers[64]. The interpretation of the first, second, and third monolayers could not be substantiated through the use of LEED or STM, as these techniques were not available. Instead, efforts were made at mapping the uptake using Low-energy Ion-scattering Spectroscopy. It was extremely important, that no sputtering of the magnesium overlayer occurred during data acquisition. Sputtering could be eliminated completely, by adjusting the ion-flux, and reducing data acquisition time. The results of the magnesium uptake,

as studied by this method, are shown in Figure 4.3. It is fairly clear, from this figure, that at a coverage around 1 ML Mg, a break point is seen, which we interpret as the start of the formation of the second monolayer. The fact that the molybdenum substrate peak, does not completely vanish, upon completion of the first monolayer, is interpreted as the fact that as the Mg overlayer is very open, some molybdenum atoms are still visible. The right panel of Figure 4.3 shows the most likely structure of the overlayer, as calculated by density functional calculations, and confirms the notion that the first 3 monolayers are, in fact, growing epitaxially on the substrate. Once the 3 epitaxial monolayers are completed, the overlayer is expected to revert to a close-packed stacking arrangement.

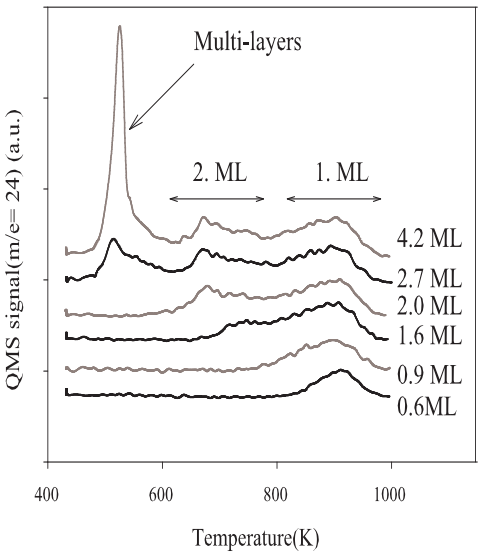

Figure 4.2: TPD spectra of Mg(m/e=24), for increasing coverages of magnesium. Coverages are normalized according to the high temperature TPD peak. A discussion of monolayer definitions is given in the text.

A typical ion scattering spectrum of a complete Mg overlayer is shown in Figure 4.4. It is especially interesting to note the very high background of helium ions scattered with kinetic energies above 550 eV. This is also seen for Al on Re(0001), and was attributed to multiple-scattering events, and neutralization and reionization events[69].

4.3.2 Formation of hydrogen overlayers

Due to the well-documented fact that simple metals lack the ability to dissociate hydrogen, we found that the atomic hydrogen adsorbed on the molybdenum substrate could be used as a limited source of hydrogen. In order to observe if atomic hydrogen was indeed being transported on to a growing magnesium film, experiments were performed to verify this, and are shown in Figure 4.5. The experiment consisted of cooling the crystal in a hydrogen backpressure, $2{\cdot}10^{-6}$ mbar, and subsequently evaporating magnesium onto the surface, at a rate around 1Å/minute. We clearly see that at 0 monolayers

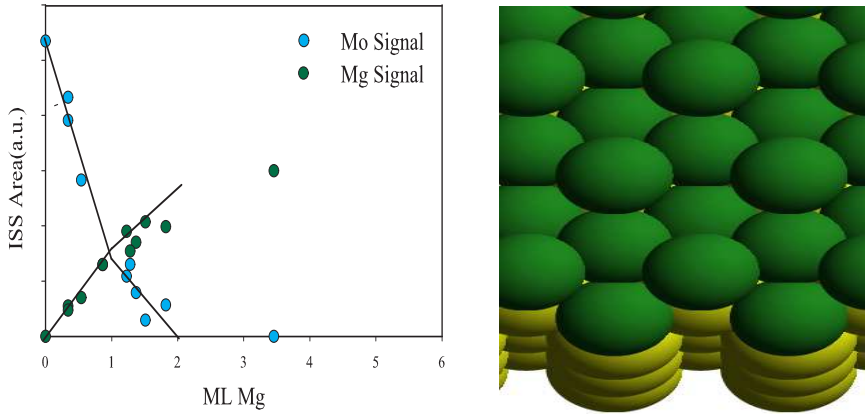

Figure 4.3: Magnesium on Molybdenum. The figure on the left shows Mg on Mo uptake, as registered by low-energy helium ion scattering. The figure on right shows density functional structure calculations, of most stable structure of 3 ML magnesium on Mo(111).

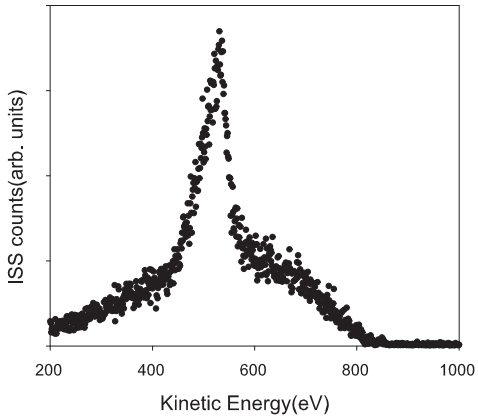

Figure 4.4: Low energy ion scattering spectrum, of magnesium deposited on Mo(111). E_p=1000 eV

of magnesium (the clean Mo crystal), only a hydrogen signal corresponding to the molybdenum crystal is seen, which adsorbs 3 monolayers of H[66]. As fractional monolayers are deposited, a drastic change in the hydrogen desorption profile is seen, due to hydrogen atoms spilling over from the molybdenum substrate to the growing magnesium overlayer. In particular, when the second monolayer is completed, a very sharp hydrogen desorption

peak emerges at 500 K, the origin of which shall be discussed later. The complexity of the hydrogen desorption profile, at intermediate coverages, between 1 and 2 ML Mg, is possible related to the formation of magnesium islands. No desorption of molecular magnesium-hydride, was observed. This could be checked by measuring a mass/charge ratio of 26 with the mass spectrometer.

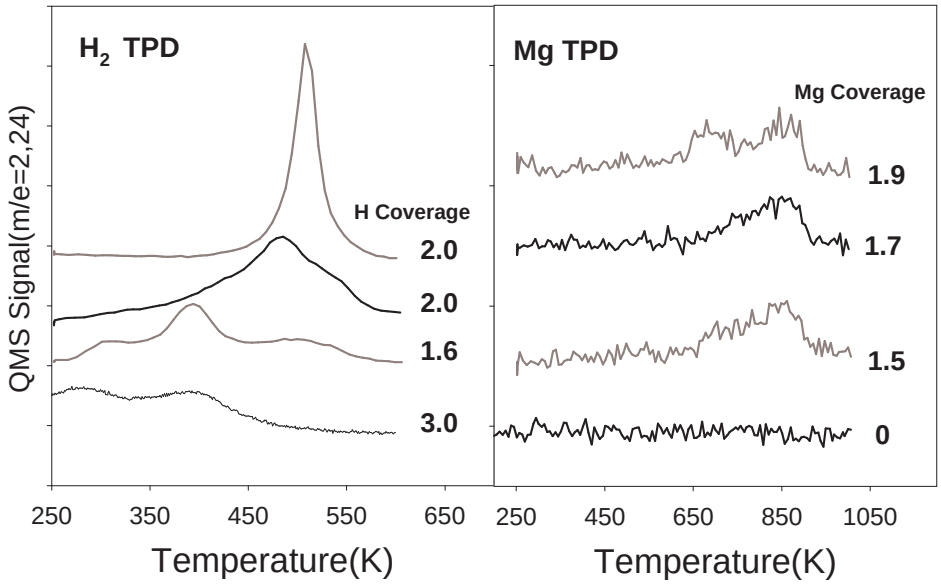

Figure 4.5: TPD spectra for hydrogen(m/e=2) and magnesium(m/e=24). Increasing Mg coverages, deposited at 253 K. Zero magnesiun-coverage experiment was performed at 135 K.

Figure 4.6 shows the TPD spectra for thicker films, which confirm that upto a coverage of around 2 ML, no hydrogen is adsorbed, other than the hydrogen adsorbed on the molybdenum crystal. As the magnesium coverage increases, the hydrogen peak shifts to 520 K, while a new hydrogen desorption feature is seen emerging between 450 K and 480 K, which is attributed to hydrogen being incorporated in the magnesium film, and bound chemically, thus forming a hydride. At the highest coverages presented in Figure 4.6, the coverage of the high temperature desorption peak, decreases by about 50 %, from 2 ML H to around 1 ML H. We believe that the following series of events describe the results.

I MgH_x films of some stoichiometry are formed during deposition at 253 K, as a result of spill-over from the active molybdenum crystal.

That MgH_x films are formed was confirmed by binding energy measurements, some of which are shown in Figure 4.7.

II As the system is heated, the MgH_x films decompose, releasing hydrogen, around 470-480 K.

III Mg sublimes around 500-520 K, leaving behind the hydrogen overlayer, which was formed at the surface during the deposition process.

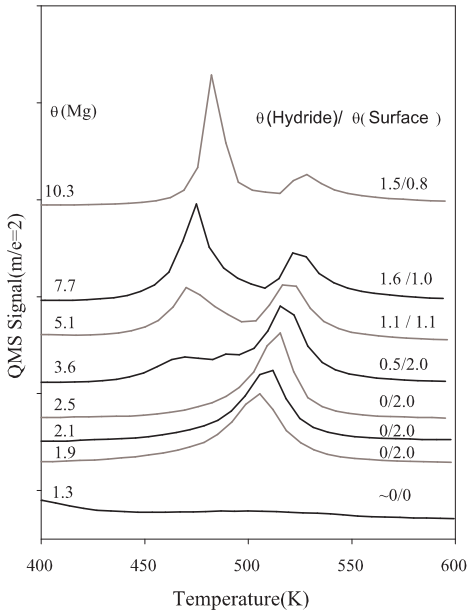

Figure 4.6: TPD spectra for increasing Mg coverages, deposited at 253 K, in a background of $2{\cdot}10^{-6}$mbar H_2

We noted that the desorption profile of magnesium was unaffected by the presence of hydrogen, which led us to believe that the structure of the Mg overlayer, as described in subsection 4.3.1 was preserved. It follows logically, that by decreasing the hydrogen coverage, i.e. increasing the deposition temperature, bulk hydride formation can be avoided completely. This is shown in Figure 4.8. We see that at temperatures above 363 K, hydride formation is eliminated, as ascertained through the absence of the low temperature hydrogen desorption peak. The results presented in Figures 4.6 can be related to the work of Sprunger of Plummer[56], who argued that a surface hydride state was formed upon hydriding a magnesium single crystal with an atomic doser. Due to the obvious problems related to magnesium sublimation, they did not perform systematic desorption experiment but noted the following:

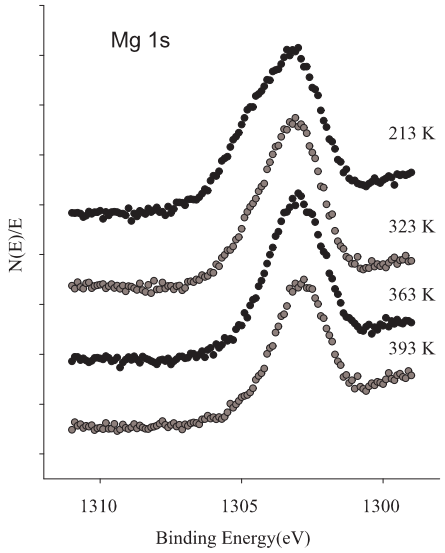

Figure 4.7: XPS of 3 ML Mg, deposited at various temperatures. hν=1486.6 eV

... H_2 begins to desorb at $\simeq$ 430 K..... continues as the Mg begins to sublimate at $\simeq$ 450 K..[By comparing to the H/Be system a desorption barrier of 1 eV is determined]. It is therefore believed that by lowering our substrate temperature, and essentially increasing the hydrogen coverage, our results mimick that which was found by Sprunger and Plummer. Our experiments had the added benefit of being able to study the desorption features, without worrying about evaporating a magnesium single crystal into the chamber, which was the reason thermal desorption was not pursued in [56].

Density functional structure calculations were performed in order to check if the magnesium overlayer structure was able to bind any hydrogen, as the desorption experiments suggested. For 2 ML magnesium thin films, a single hydrogen overlayer is found to be unstable, whereas 2 ML of hydrogen is stable. For 3 ML magnesium films, the molybdenum substrate is screened, and a significant shift of the stability of a single vs. the 2 ML configuration is observed, favoring a single monolayer of hydrogen being adsorbed. A possible explanation for the observed shift in stability of the adsorbed hydrogen overlayer, desorbing around 520 K, can therefore be found with density functional calculations. The calculational results are summarized in Figure 4.9. For calculational details, the reader is referred to Paper I.

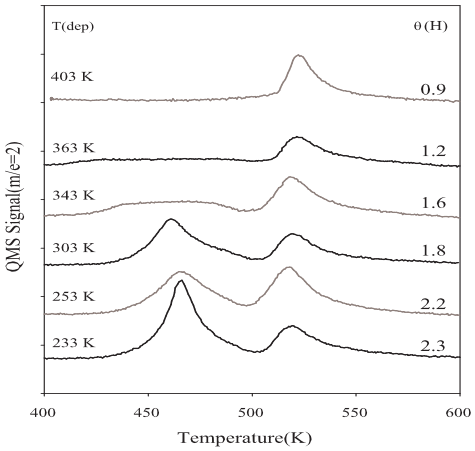

Figure 4.8: Hydrogen TPD spectra(m/e=2). Mg films (5 ML), deposited in $2{\cdot}10^{-6}$ mbar H_2, at different temperatures. θ(H) is given as the sum of H adsorbed as overlayer and hydrogen bound as hydride.

4.3.3 Hydriding with atomic hydrogen source

Given the limitation of the amount of hydrogen available to the magnesium film, described in section 4.2, it was clear that an alternate source of hydrogen was to be employed, in order to hydride thicker Mg films. A generic, low-effiency, filament doser was used in this endeavour. By mounting the filament out of sight of the crystal, some effiency was lost. However, tungsten evaporation onto the crystal could be eliminated. In order to perform atomic hydrogen doses, which didn't contaminate the surface with oxygen, a heavy outgassing procedure was carried out, consisting of outgassing the doser at 100 W in a partial pressure of $2{\cdot}10^{-5}$ mbar hydrogen for several hours, prior to use. Furthermore, the hydrogen gas used was cleaned with a catalyst and molecular sieve. It was found that after a 30 minute dose, no further hydride formation was observed upon hydriding a 12 ML Mg film. This was observed by an investigation of the Mg 1s line, where the extent of hydride formation could be monitored non-invasively. Figure 4.10 shows hydrogen desorption spectra obtained after hydriding various film thicknesses of magnesium, for 30 minutes at 343 K. The thinnest films, with thicknesses below 2 ML, do not appreciably adsorb any hydrogen, nor form the chemical hydride phase. As the thickness increases, we note an increase in the stability of the hydrogen bound in the hydride phase. The stability of the hydride relative to the magnesium overlayer was investigated by simultaneous mea-

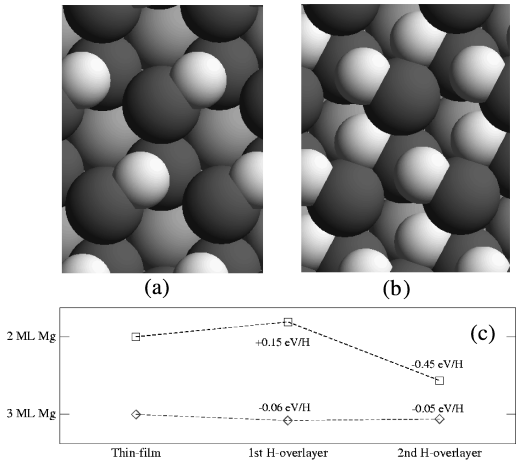

Figure 4.9: DFT calculations show that a single hydrogen(white) overlayer on a 2 ML Mg thin film (a) is unstable, whereas 2 ML hydrogen (b) is stable; the light grey atoms are the Mo substrate. For 3 ML Mg, a significant shift in the stability of a single vs. 2 ML hydrogen overlayer is observed, where the single hydrogen overlayer becomes stable(c), and the stability of the 2nd layer is reduced. From Paper I.

surement of the magnesium and hydrogen signal, from a 12 ML Mg film, exposed to atomic hydrogen. This is shown in Figure 4.11. The difference in intensity can be understood by appreciating that the two different elements have very different probabilities of being detected in the mass spectrometer. Mg atoms, desorbing from the crystal surface, will only be detected if the trajectory is such that it is not adsorbed on the interior of the wall leading to the ionization unit.

Hydrogen, however, will scatter off the walls several times, irrespective of the trajectory, and hence will be detected more easily. The position of the hydrogen and magnesium peaks suggest that the hydride phase is just as stable as the metallic film. Therefore it seems that magnesium sublimation is a prerequisite for hydrogen release.

Temperature-programmed XPS was performed, on a hydrided magnesium film, in order to try to understand the results from Figure 4.11. From Figure 4.12, we see a gradual collapse of the initially split Mg 1s line, due to the decomposition of the hydride phase, which, at this slow heating rate,

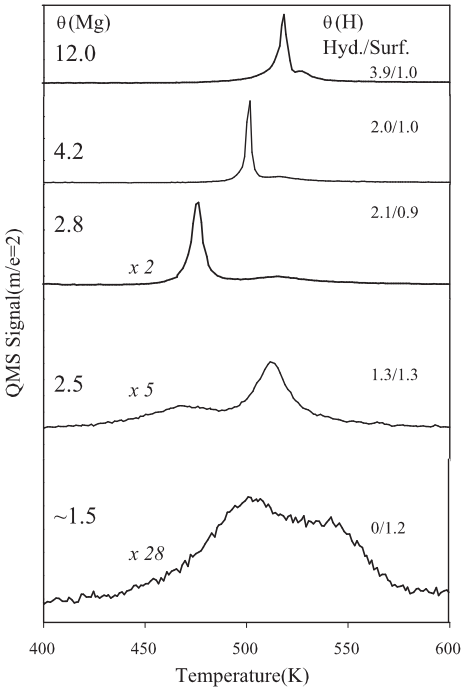

Figure 4.10: Hydrogen TPD graphs after hydriding various magnesium film thicknesses with 30 minutes of atomic hydrogen, at 343 K. *Note the scaling factor*

does not result in a desorptive loss of magnesium. The results from Figure 4.11 and Figure 4.12 can be explained by the fact that the system is not in equilibrium during a TPD experiment and the observation that the hydride formation seems to be self stabilizing as seen in Figure 4.10 where the peak was observed to shift towards higher temperatures when the Mg grew thicker and hydride concentration increased. If we on the other hand heat very slowly and wait long enough some decomposition will eventually occur. If this rate is sufficient some hydrogen can desorb and the rest will be destabilized and desorb at a much lower temperature. Experiments have shown that if a metal-hydride film is formed and left at around 416 K, hydrogen desorption does indeed occur after 2 minutes. The results of the isothermal desorption are shown in Figure 4.13. It is not clear why there are two desorption peaks, as a function of time.

Temperature-programmed XPS, has also been performed by Fischer and co-workers[59], who found, for a magnesiun film deposited on top of a hydrided palladium foil, a similar collapse of the Mg 1s line, upon heating.

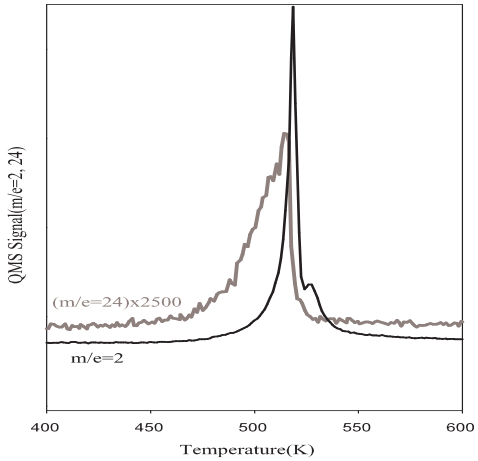

Figure 4.11: TPD spectra of Mg and H_2 signals, from a 12 ML MgH_2 film, formed with an atomic hydrogen doser.*Note the scaling factor*

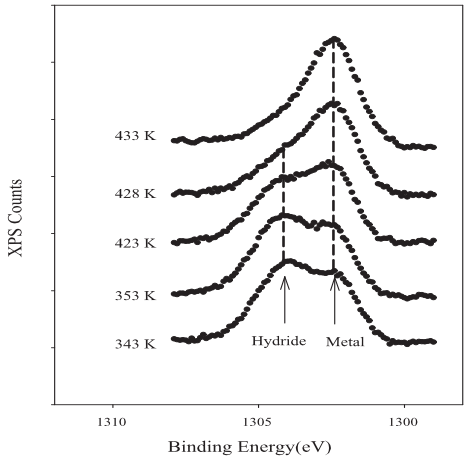

Figure 4.12: XPS spectra of the Mg 1s line for a hydrided Mg film, obtained at different temperatures. hν=1486.6 eV.

However, due to the possibility of alloying and intermixing, it is not clear if the collapse was due to onset of alloying or intrinsic hydrogen release from magnesium. The authors note that they believe that an intermetallic compound was formed between palladium and magnesium, following hydrogen desorption.

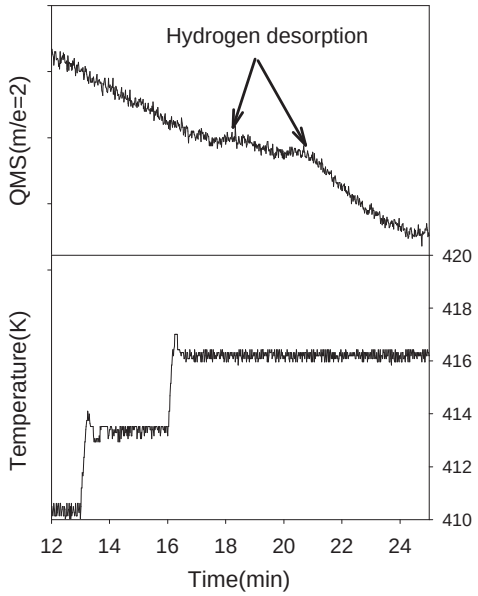

Figure 4.13: Isothermal desorption of hydrogen, from 12 ML magnesium hydride film, formed by means of an atomic hydrogen doser.

4.4 Conclusions

The main results of this chapter are summarized below.

- Hydrogen overlayers could be adsorbed on the surface of magnesium, through simultaneous dosing of hydrogen and evaporation of magnesium at low temperatures. This is presumably due to molecular hydrogen being dissociated at the surface of the molybdenum crystal, and being transported onto the surface of the growing magnesium film, through a spill-over effect. This overlayer was approximately quantified, and a saturation value of 2 ML H for 2 ML of magnesium was found. For thicker magnesium films, the saturation value decreased to 1 ML H. This could be confirmed by density-functional calculations.

- Magnesium hydride formation was seen when evaporating magnesium in a hydrogen background, at temperatures below 363 K, again through a spill-over effect.

- The magnesium hydride was found to be self stabilizing. At the highest hydride contents, the desorption of magnesium and hydrogen was simultaneous, as witnessed by a TPD experiment.

The fact that substantial temperatures are needed (500-520 K for the surface overlayer and 470 K for the hydride phase) to release the hydrogen from magnesium hydride is in good agreement with the problems encountered using magnesium as a hydrogen storage medium, as discussed in the introduction. To relate our findings to lab-scale magnesium-based storage systems, we find it remarkable that the sublimation of magnesium, witnessed in vacuum, during hydrogen desorption does not incur serious cycling losses in ball-milled powders. The nanoparticles should undergo substantial sintering under these conditions, thereby agglomerating into large particles with strong diffusion limitations, and a loss of surface area. We suggest that significant levels of MgO, which are often present in these high area hydrogen storage media, help stabilize the nanoparticles, but at the same time inhibit the kinetics of hydrogen uptake and release. In subsequent chapters, the exact role of magnesium oxide is investigated, which reveal some interesting, novel features.

While a strong point can be made that the results of the first part of these investigations(which are exclusively an artifact of the molybdenum-magnesium interaction) are not exactly relevant to the topic of hydrogen storage, the work was pursued as it provided an elegant link between well-defined experiments conducted on a model-system scale and quantum mechanical structure calculations. Structural investigations, either through the use of scanning-tunnelling microscopy or LEED could, of course, have strengthened the scientific foundation of the work, but was not pursued. A result, which could be applied directly, concerned the desorption of metallic magnesium and gaseous hydrogen, which desorbed in unison, in the simplest well-defined system.

CHAPTER 5

MgO overlayers

This chapter covers some of the investigations of the effect of magnesium oxide on the hydrogen storage properties of magnesium. In Chapter 4 we found, by studying the simplest model system, that the demand for cyclic stability, shown in Table 1.1 on page 7, cannot be fulfilled for metallic magnesium films, grown epitaxially on a molybdenum single crystal. Therefore, we attempt to extend our understanding of the system, by including the presence of an oxide contaminant, which is hard to avoid in powder samples, as these have, in general, been exposed to air. In this chapter we argue that the presence of magnesium oxide in the system is a prerequisite for cyclic stability.

5.1 Temperature Calibration

During the course of the experiments, there was a change of sample holder, which promptly introduced a shift in the temperature on all desorption peak. In this section, a calculation is given, which underlines that the second sample holder reads out the correct temperature, while the first sample holder was off by 28 K.

Mg evaporation

The rate of change in magnesium coverage during a thermal desorption of experiment is given as

$$\frac{d\theta}{dt} = \frac{P_{eq}}{N_0\sqrt{2\pi m_{Mg} k_B T}} \tag{5.1}$$

where P_{eq} is the temperature dependent equilibrium pressure, N_0 is the surface density of Mg(0001), m_{Mg} is the atomic mass of Mg, T is the temperature, and k_B is Boltzmann's constant. The equilibrium pressure of magnesium can be expressed empirically as

$$\log_{10}(P_{Mg[Pa]}) = 5.006 + 8.489 - \frac{7813}{T} - 0.8253 * \log_{10}(T) \qquad (5.2)$$

By inserting the value of the equilibrium pressure at different temperatures, we can simulate a TPD of metallic magnesium, and compare it with obtained data.

Figure 5.1: Simulated TPD and Mg TPD curves from 2 different sample holders of Mg films. β=3K/s

We see, from Figure 5.1, that there is general agreement, as a result of using Equation 5.1, and renormalizing the TPD data to units of monolayers desorbing. Also shown are the data with the old sample holder, which illus-

trate the apparent disagreement. The Mg films, investigated in Chapter 4, were substantially thinner, as is shown.

5.2 Introduction

The study of magnesium for hydrogen storage applications is, in general, studied through the use of mechanical alloying, in order to reduce particle size and facilitate alloy formation, as mentioned in Chapter 2. It is also believed, that ball-milling introduces defects which serve as diffusion paths for atomic hydrogen[32]. Characterization of these systems, is done by performing non-surface sensitive analysis, like volumetric hydrogen uptake, X-ray diffraction, TEM and EDX(Energy Dispersive X-ray Analysis) investigations. Characterization by XRD and EDX cannot, in general, reveal any oxygen content[1], despite the fact that the powders have been exposed to air for prolonged periods of time. The TEM/EDX equipment used, for example, in [32] and [33] is equipped with a Be window, and is therefore not able to see oxygen. Shao and co-workers[71] prepared ultra-fine magnesium nanoparticles, by a metal-plasma reaction, with an average particle size of 300 nm. They found complete hydrogenation at 673 K, in 60-70 minutes, at 40 bars, which is the fastest uptake measured for non-catalyzed and non-activated magnesium powders, and compares to catalyzed magnesium systems. Subsequent hydrogenation cycles were much faster, with complete hydrogen uptakes achieved in 10 minutes. What is clear from this investigation, is that swift hydrogen uptake was observed, despite the obvious presence of an oxide overlayer, estimated to be around 1%. The oxide overlayer was formed in a mixture of argon and air, over a duration of 24 hours, in order to prevent powder combustion as the powder samples were transferred from the preparation chamber to the analysis chamber. Investigations of the MgH_2-V-Ti composite, by Dehouche and co-workers[72], revealed that upon adding 101 ppm moisture to the hydrogen gas, a slow-down in desorption kinetics was found while no effect on absorption was found.

Hjort and co-workers have studied the effect of oxygen on the hydriding mechanism of well-defined palladium-coated magnesium films, and found that, at moderate oxygen concentrations, the hydrogen uptake rate increased, and was reduced again at increasing oxygen concentrations [73]. Interestingly, in their experiments, the uptake never decreased to zero, which hinted

[1]The entrance window, used in these systems is generally made of beryllium, which only allows transmission of X-rays greater than 1 keV, i.e. elements heavier than Na. XRD will also have trouble finding a thin oxide layer, due to linebroadening, from the Debye-Scherrer effect. Furthermore, an amorphous oxide phase will not be visible either.

at finite diffusivity, even at temperatures below 375 K. The cause of the increased hydrogenation rate was suggested to be related to the formation of nucleation sites for the hydride phase. The effect on the thermal desorption properties on hydrogen was not investigated, due to the complication that heating the system led to Pd-Mg alloying.

Yoshimura and co-workers have similarly studied the Pd-Mg thin film system, and found considerable hydrogenation of the magnesium film, in 5 seconds, even at room temperature. Sputter profiles revealed, furthermore, that a vast amount of oxygen was present in the magnesium film, which could have affected the hydriding kinetics[53]. Given the reactive nature of metallic magnesium, it is difficult to completely avoid thin shells of MgO being formed at the surface, when using powders for hydrogen storage. As mentioned in Chapter 2, heavy activation of magnesium is usually required, before any hydrogen uptake is observed, depending on sample quality. Andreasen and co-workers[47] have recently compiled a selection of hydrogenation/dehydrogenation data for a number of magnesium samples, and found a considerable spread in activation energies. Activation energies between 70 kJ/mol and 300 kJ/mol were found, for both hydrogenation and dehydrogenation reactions. This spread in energies was attributed to differences in sample purity, in particular the formation of a protective oxide shell around the metallic particles. The diffusion of atomic hydrogen in ceramics, like MgO, is very slow. Gonzalez and co-workers[35], have found hydrogen diffusion to be measurable only at temperatures above 1750 K, indicating that at hydriding temperatures(between 600 K and 700 K) hydrogen permeation through a perfect oxide will not proceed. UHV investigations concerning the oxidation of magnesium have been carried out by several groups[64, 74, 65] on molybdenum and ruthenium surfaces. Fournier et al have also studied the magnesium oxidation at elevated temperatures, at oxygen pressures of 20 kPa[34]

5.3 Experimental Background

To illuminate the effect of magnesium oxide on the hydrogenation and dehydrogenation properties of magnesium, we initiated a surface science study with this focus. In particular, given the results of Chapter 4, and our wish to build a bridge between model-system investigations, and the real powder-based system, we were keen to see if magnesium oxide could explain our inability to obtain cyclic stability of well-defined systems in vacuum. The kinetics of oxide formation were studied indirectly, by evaporating a clean magnesium film onto the quartz crystal microbalance, and monitoring the

time-dependent increase in deposited mass, upon oxidation. Although we cannot be exactly sure that the magnesium film on the QCM reliably mimicks the corresponding film on the molybdenum single crystal, the qualitative behaviour should be directly transferrable. Furthermore, by combining the results of the QCM with other methods, like low-energy ion scattering, some continuity can be established.

5.3.1 Experimental Details

The experiments in this chapter consist of evaporating magnesium films onto the metallic molybdenum substrate for characterization. However, to aid us in the kinetics of oxide formation, we also use the quartz crystal microbalance, for real-time logging of the oxidation process. As the QCM cannot be cleaned in vacuo, relatively thick magnesium films (100 Å) were evaporated for each new oxidation experiment. This thickness was found to be sufficient to eliminate memory effects from the previous experiment.

5.3.2 Oxide quantification

To quantify the oxide thicknesses with which we are working, we utilize an indirect approach, allowing us both to study the kinetics of oxide formation at different pressures, and, more importantly, quantify the oxide thicknes. This approach consists of evaporating set thicknesses of magnesium onto the QCM, and studying the kinetics of oxidation at various oxygen pressures.

The magnesium oxidation process is known to be self-limiting. The limiting oxide thickness is reported to be around 12 Å after oxygen exposures of $1{\cdot}10^{-6}$ mbar for 120 s[51], for well-defined magnesium films. The kinetics of oxide formation are also reportedly consistent with a nucleation and growth mode[51, 62]. The oxygen uptake results obtained by us are presented in Figure 5.2, for different oxygen pressures. After an initial sigmoidal uptake, a growth stage ensues which can be described by inverse logarithmic kinetics[75].

When interpreting uptake measurements, describing the kinetics of oxidation, we note that the mass increase observed is a measure of total oxygen absorption, while the extent of oxide formation can be indirectly evaluated through a calculation of the amount of magnesium consumed. In this case, assumptions about stoichiometry must be made. When stating the thickness of an oxide layer, we always assume 1:1, i.e. MgO, stoichiometry. Assume that a mass increase, ΔM, is observed, upon oxidation. The amount of Mg consumed is thus $m(Mg) = \Delta M \cdot \frac{24g/mol}{16g/mol}$. The thickness of the MgO layer can then be calculated from the density of stoichiometric MgO, $\rho(MgO)$ =3.58

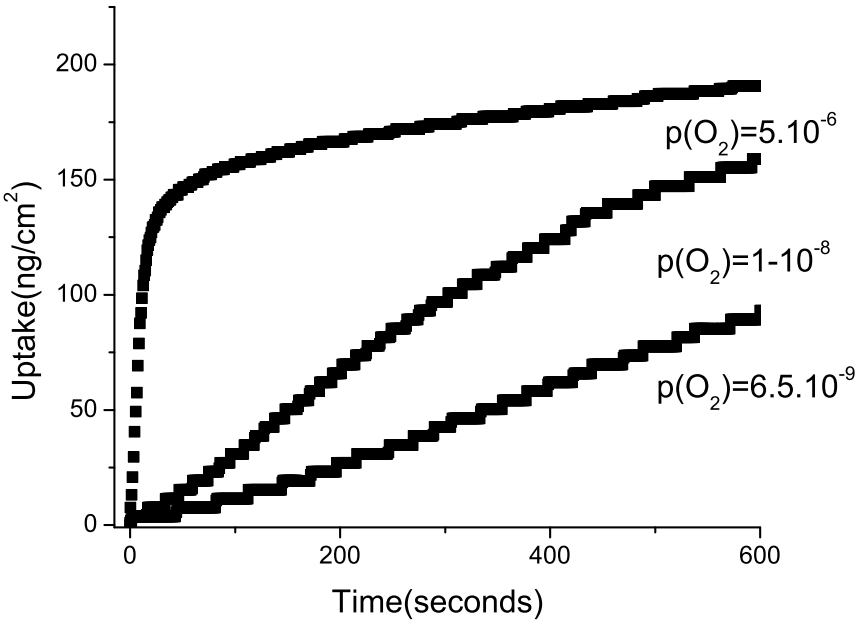

Figure 5.2: Nucleation and growth of magnesium oxide film, as monitored by the QCM, at different partial pressures of oxygen. T=300 K.

g/cm^3, i.e.

$$T(MgO[\mathring{A}\ ]) = \Delta M[g/cm^2] \cdot \frac{1 + \frac{24g/mol}{16g/mol}}{3.58g/cm^3} \tag{5.3}$$

We see that after exposing the film to $5{\cdot}10^{-6}$ mbar O_2, a limiting oxide thickness around 14 Å is formed, in agreement with similar experiments[51].

We have also studied the formation of stoichiometric MgO films, and the effects on hydrogen desorption, by evaporating the magnesium films in a partial pressure of oxygen. Using the QCM, we are able to reliably ascertain the required oxygen pressure, for perfect stoichiometry. The uptake is shown in Figure 5.3. We see that at pressures above p=$1{\cdot}10^{-7}$ mbar, stoichiometric films are formed. This is clear from the inset in Figure 5.3, as the uptake rate becomes constant at higher oxygen pressures. This is agreement with, for example, Wu et. al[64].

If we examine the slopes of the incremental mass increase for the metallic and stoichiometric oxide films, in Figure 5.3, we should expect the ratio of the slopes to be $m(MgO)/m(Mg) = 1.66$. However, we observe a difference of 12 % compared to the ideal value. This is probably due to differences in

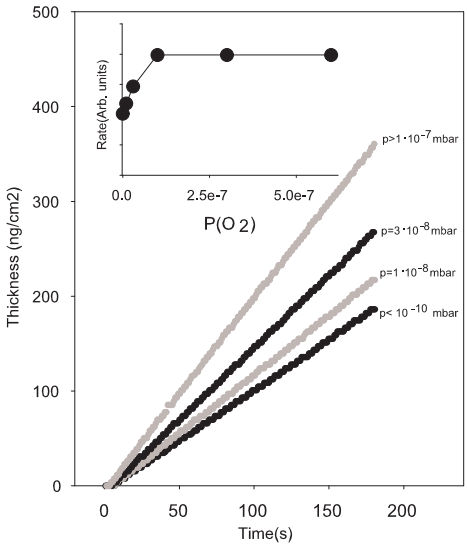

Figure 5.3: Evaporation of magnesium in different partial pressures of oxygen, yielding different compositions of magnesium oxide. The inset shows the uptake rates, as function of oxygen pressure. At pressures above $1{\cdot}10^{-7}$ mbar O_2, stoichiometric MgO films are formed.

the acoustic impedance of magnesium and magnesium oxide[76]. We have, in the above discussion, assumed that the mass increase is linearly related to the frequency shift, which introduces a slight error.

Magnesium Oxidation: XPS

The extent of magnesium oxidation was also studied by investigating two different photoelectron lines for magnesium, when exposed to $2{\cdot}10^{-6}$ mbar O_2 for 30 s, 150 s, and 480 s. The Mg 1s line is the most surface sensitive line available, with inelastic mean free path of 10 Å and hence probes the outermost atomic layers. The Mg 2p line has an escape depth of 20 Å and hence contains contributions from the bulk[77]. Figure 5.4 shows the evolution of the Mg 1s and Mg 2p signals at increasing oxygen exposures. It is clear, from the left panel in Figure 5.4 that the surface oxidizes immediately, while the Mg 2p line, reveals that the bulk of film is not completely oxidized. A broadening of the Mg 2p line is seen, due to the emergence of a peak due to oxidized Mg. Analysis of the O 1s line(not shown), reveals, for the completely oxidized surface, a sharp feature at 531.0 eV, in perfect agreement with, for example, Fournier et. al.[34].

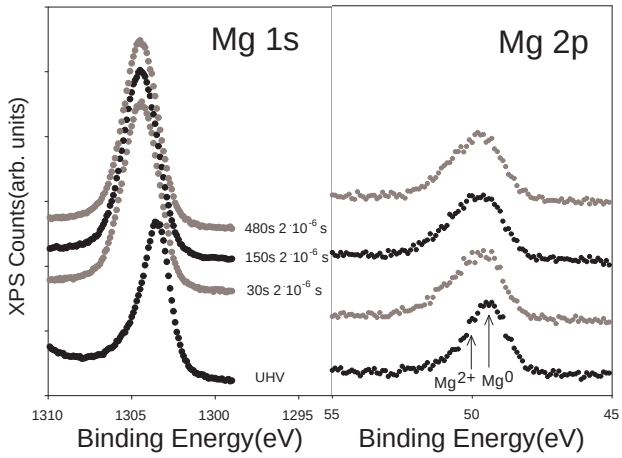

Figure 5.4: Oxidation of 100 Å Mg at room temperature, monitored with XPS. hν=1486.6 eV

5.3.3 Surface Structure

Magnesium films were then evaporated onto the surface of the single crystal molybdenum substrate. To study the surface structure of oxidized magnesium, ion-scattering was used. Ion scattering is an extremely surface sensitive technique, capable of probing only the outermost atomic layer. By post-oxidizing a magnesium film, in $1{\cdot}10^{-8}$ mbar O_2 and henceforth recording ion scattering spectra, we can study the surface composition of the outermost layer, as well as estimate the oxygen dose after which further surface oxidation ceases. Figure 5.5 shows evolution of the magnesium and oxygen signals as function of time. From Figure 5.5, we clearly see that the magnesium signal does not vanish, upon increased oxidation. This agrees well with the sodium chloride structure of MgO. Figure 5.5 also shows the mass increase observed in the parallel experiment, performed on the QCM. We see that after 200 s oxygen exposures, in $1{\cdot}10^{-8}$ mbar O_2, the magnesium and oxygen signals level out, at a constant value. From the kinetic data obtained from the QCM shown in the same plot, we see that continued oxidation proceeds, into the bulk of the film. It should be mentioned, that the ion scattering actually suggest that the growth mode consists of monolayer formation, followed by 3D growth. However, QCM uptake data clearly suggest a sigmoidal uptake, indicative of nucleation and growth kinetics, and due to the the poor resolution of the ion scattering data, the QCM data appear

more reliable.

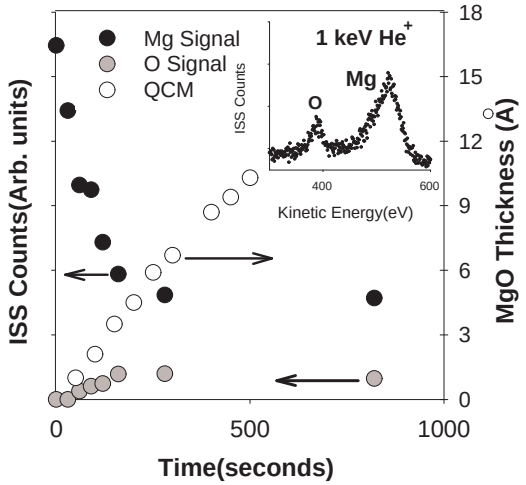

Figure 5.5: He^+ ion scattering data, showing magnesium and oxygen signals as function of oxygen exposure time. Also shown is the uptake curve for oxygen on magnesium. as recorded by the QCM. $P(O_2)=1\cdot10^{-8}$ mbar). Inset MgO_x ISS spectrum

5.3.4 Intermixing

We also investigated the properties of a 30 Å magnesium film evaporated onto a post-oxidized magnesium film, of thickness 14 Å such that the thermal stability of the system could be probed. This is shown in Figure 5.6, by tracking the Mg 1s line, with the Al Kα line, at different temperatures. At the lowest temperatures, a clear split of the line is seen, with the feature at 1303.7 eV being the most prominent. As the system is heated, the feature at 1304.7 eV grows in intensity, suggesting either thermally activated diffusion of magnesium into the MgO film, or a covering of the metallic overlayer by the oxide. The latter is more likely, due to the lower surface energy of the oxide component[78].

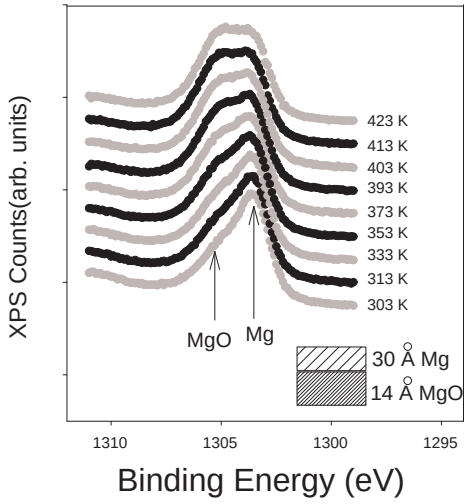

Figure 5.6: XPS. Mg 1s line. Heating rate is approx. 4 K/min. Obtained with Al Kα source, hν=1486.6eV.

5.3.5 Thermal Stability

To study the effect that a magnesium oxide overlayer has on the desorption properties of the metallic sub-surface magnesium film, we oxidized 70 Å Mg films, which we were certain would not oxidize completely, based on the results from the QCM presented in Figure 5.2. Oxygen exposures consisted of 1000 s dose at 393 K, at p(O_2)=5·10^{-8} mbar and 5·10^{-7} mbar. The thermal desorption spectra of these 70 Å Mg films are shown in Figure 5.7, and clearly show that the magnesium peak is shifted upwards, at increasing oxygen exposures. The desorption curves shown in Figure 5.7 have been renormalized, such that the amount of metallic magnesium is constant. The integrated intensity of the oxide-capped magnesium films, corresponding to the m/e=24 signal, was found to be 20 % less than the non-oxidized films, consistent with the formation of approximately 14-15 Å of MgO. MgO desorption is not visible in the temperature range presented here. MgO has been shown to thermally decompose at temperatures above 1300 K[64]. The thermal desorption was not investigated here, due to limitations in the Mo crystal mount, which prevented regular heating of the crystal to these high temperatures. A few experiments were carried out, however, which confirmed the decomposition of MgO on the surface.

Figure 5.8 shows the results of an Arrhenius analysis of the zero-order

desorption of magnesium TPD experiments shown in Figure 5.7. The increase in apparent desorption energy, from 140 kJ/mol to over 300 kJ/mol, agrees qualitatively well with the results of Chen and co-workers[36], who observed cracking of the magnesium films at temperatures above 400^{o}C. The oxide component in their work, was presumably substantially thicker than the oxide thicknesses formed here, thereby requiring higher temperatures.

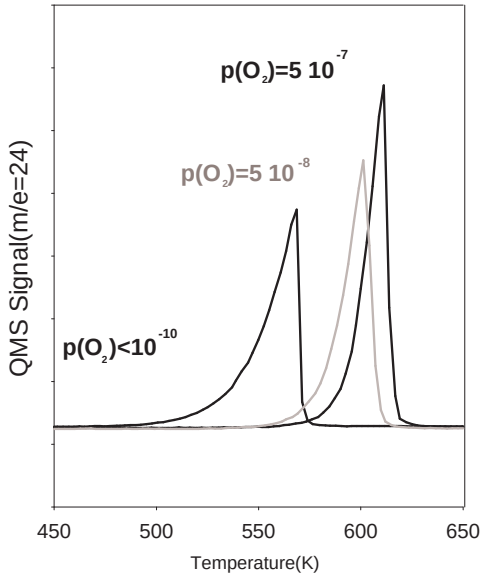

Figure 5.7: Thermal desorption spectra, for 70 Å magnesium films, illustrating the effect of capping, as a result of surface oxidation. Films were deposited at 393 K, and oxidation time was 1000 s. Desorption curves have been renormalized, as described in the text.

5.3.6 Effect on hydrogen desorption

In Chapter 4, we reported the thermal desorption behaviour, of magnesium-hydride films, formed by means of an atomic hydrogen doser. As was clear from this work, hydrogen desorption was accompanied by metal sublimation, which made us question the cyclic stability of magnesium for storage purposes. We therefore tried to model a magnesium hydride particle, with an oxide shell on top.

A hydride film was formed, by hydriding a 90 Å magnesium film with an atomic hydrogen doser, at 343 K, and subsequently evaporating a stoichiometric MgO lid, of thickness 27 Å. By depositing magnesium in an oxygen

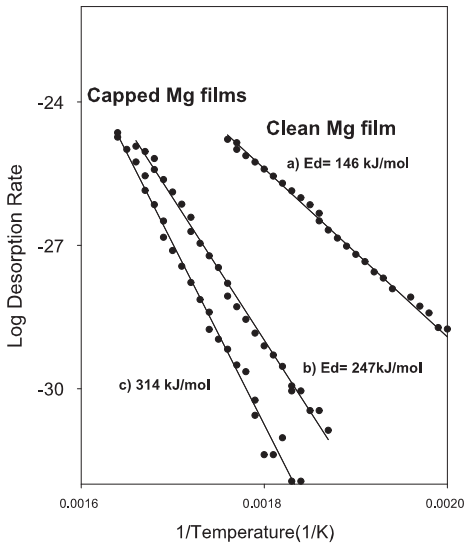

Figure 5.8: Arrhenius plots obtained from TPD spectra of Magnesium, presented in Figure 5.7. a) Mg film formed in $p_{O_2} << 1 \cdot 10^{-11}$ mbar. b) Mg film, post-oxidized $5{\cdot}10^{-8}$ mbar, 1000s. c) Mg film, post-oxidized $5{\cdot}10^{-7}$ mbar, 1000s.

pressure of $1{\cdot}10^{-7}$ mbar, we were sure of a 1:1 stoichiometry, as described in Figure 5.3. The atomic hydrogen dose was 30 minutes, at 40 W, in a hydrogen pressure of $1{\cdot}10^{-4}$ mbar H_2. The results of the hydrogen and magnesium desorption are shown in Figure 5.9. The result from Chapter 4 is included for convenience. We see, very clearly, that apart from the obvious effect of immobilizing the metallic magnesium, the hydrogen seems to diffuse through the oxide overlayer, before the magnesium. Exploiting the knowledge that the oxide thickness encountered in powder systems (160Å for the samples of Ref.[79]) are much thicker than those which are compatible with spectroscopic analysis, the kinetic barrier encountered in powdered systems, could be related to hydrogen diffusion through an unavoidable oxide overlayer. This would support the cyclic stability encountered in powder systems, for example [80, 79]. The magnesium hydride film used in the capping experiment is substantially thicker(90 Å) than the films which were used in Chapter 4. This could explain the large difference in hydrogen which desorbs, in Figure 5.9, despite the same atomic hydrogen dose.

The experiments presented in this chapter, helped to bridge the gap which emerged in Chapter 4, where we were intrigued by the seeming in-

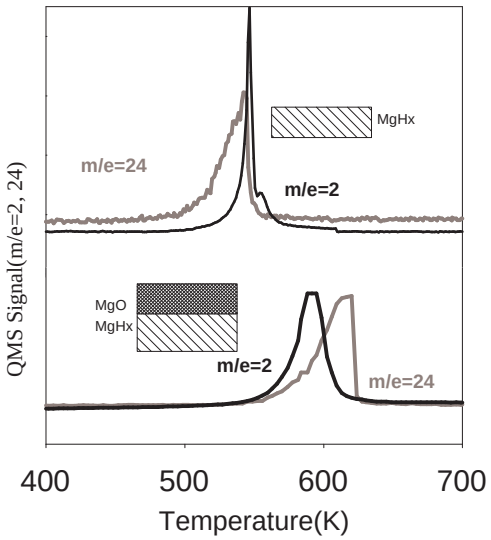

Figure 5.9: Magnesium/Hydrogen Desorption curves. Hydride phase formed with atomic doser, and capped with a 27Å MgO film. Top panel shows results from Chapter 4, which have been corrected for the temperature anomaly. θ_H(Capped film)= 16 ML H. θ_H(Non-capped)=4.9 ML H.

compatibility between what was measured under controlled conditions, and what is measured in a hydrogen storage rig, consisting of hydrogenation/ dehydrogenation cycles at temperatures above 600 K. The introduction of oxygen as an impurity seems to offer a likely explanation for the cyclic stability observed in powder-based magnesium systems. It was clear, from Figure 5.7, that the apparent desorption temperature and desorption energy of magnesium increased drastically upon oxidation. In a powder-based system, the oxide content is likely to an order of magnitude higher, thus resulting in an even more pronounced capping effect. Hydrogen permeation through magnesium oxide overlayers has been found to be finite, by Hjort and co-workers[73]. These overlayers were all formed by post-oxidation, which means that a bulk 1:1 stoichiometry is not guaranteed. Hydrogen diffusion through perfect MgO crystals was found to be negligible, at temperatures below 1700 K[35]. They found that the diffusion was markedly improved through the introduction of lithium into the system.

The differences in thermal expansion coefficients ($26{\cdot}10^{-6}$1/K for Mg vs. $10.8{\cdot}10^{-6}$1/K for MgO) are not large enough such that they might explain the observed effect on the apparent desorption energy. If, the behaviour was

indeed consistent with a mechanical cracking of the oxide overlayer, we would expect an instantaneous desorption, as opposed to the zero-order behaviour observed.

The results presented here suggest that an oxide contaminant should exert a stabilizing effect in a magnesium-based storage system, such as the ones presented by Refs.[32] and [71]. Particularly, the results suggest that an oxide contaminant, in principle, should be necessary, in order for cyclic stability to be achieved. Thus, the oxide layer has a vital role in the system, primarily as a structural promotor. Ultimately, it would seem that the diffusion behaviour of hydrogen in magnesium oxide phases is to be understood in greater detail, if magnesium-based systems are to be improved.

5.4 Conclusions

The following results have been established, using surface science investigations of thin Mg films

- Post-oxidizing Mg films increases the apparent magnesium desorption energy from 146 kJ/mol to 314 kJ/mol.
- Magnesium oxide overlayers serve as a cap, preventing magnesium sublimation, and attenuate hydrogen desorption.
- Magnesium oxide, if present in a magnesium-based storage, should promote the structural integrity of magnesium particles. Therefore, it appears to be a necessity in order for cyclic stability to be realized.

CHAPTER 6

High Pressure Experiments

In this chapter, we extend our investigations to include high pressure experiments.

6.1 Introduction

Chapters 4 and 5 illustrated that the simple view of hydrogen dissociating on a planar magnesium surface, and forming a hydride, perhaps does not adequately describe what is going on inside powder-based samples, which, we suggest will always contain a certain amount of oxide impurities. By extending the discussion to encompass high pressure and higher temperatures, we approach realistic conditions.

6.2 Experimental Background

As described in Chapter 2, all previous research with model systems in the form of magnesium thin films have consisted of the investigation of hydrogen uptake in palladium covered magnesium films[43, 50, 51, 52, 53, 54, 55, 59, 81]. Due to the complication that palladium and magnesium form an alloy at practical temperatures, and some conflicting results concerning the exact rate of uptake[43, 53], we decided to measure the sticking coefficient, once and for all, on pure magnesium films directly, supported on a non-alloying substrate, and in that way avoid the complication related to alloying entirely. Also, as we can avoid the temperature barrier imposed by the onset of alloying, described in [52], the effect of temperature on sticking probabilities

Diffusion Constant	Temperature	x_{100s}	x_{1000s}	Reference
$9.7510^{-11}m^2/s$	300 K	139 μm	442 μm	[41]
$2.4510^{-9}m^2/s$	450 K	700 μm	2200 μm	[41]
1.1 $10^{-20}m^2/s$	305 K	0.001 μm	0.005 μm	[43]

Table 6.1: Diffusion Constants, at various temperatures. Diffusion lengths are also given.

can be reliably measured, thus yielding an activation energy for hydrogen dissociation. However, from the results in Chapter 4, we see that the maximum hydriding temperature is ultimately determined by the temperature at which the evaporation rate of magnesium becomes substantial.

Table 6.1 lists some of the available diffusion constants, for hydrogen in magnesium, calculated for different temperatures, and times, using the relationship, $x_{1/2} = \sqrt{2Dt}$, for the average diffusion length, given a diffusion length, D and time, t. We see that the diffusion constant for overall hydride formation, measured by Spatz and co-workers[43], is extremely low, which means that diffusion will always present a problem for all but the smallest magnesium particles. From the work presented in [43], it is not clear if the extremely low diffusion constant is a consequence of the formation of an interfacial hydride, created at the palladium-magnesium interface.[1] In any case, if hydrogen is dissociated at the surface of a magnesium film, we should not experience hydrogen transport limitations, due to diffusion, according to [41]. From Table 6.1, we see that atomic hydrogen will diffuse at least 5 nm, in the space of 1000 s, i.e. around 20 ML of Mg. On the basis of the reported dissociate sticking coefficient for hydrogen on magnesium[39] of 1.6 $\cdot 10^{-11}$ at room temperature, we can estimate that, within the timeframe of a hydrogen dose around $1 \cdot 10^{12}$ ML, only 10 ML of hydrogen will dissociate at most. Therefore, sticking should be rate-limiting in these experiments.

To roughly estimate the extent of hydride formation, XPS measurements were performed after the high pressure hydrogen exposure, some of which are shown in Figure 6.1. The figure shows little chemical shift due to the formation of the hydride, or β-, phase. At the highest temperatures, 423 K, some indication of hydride formation is clear, as a shoulder on the high binding energy side. We see that the hydrogen content is much smaller than that which was shown in Figure 3.1 on page 21.

[1] In the proposed model, hydrogen diffusion is proposed to occur only through the non-hydrided part of the sample, i.e. a smaller effective area for diffusion is available.

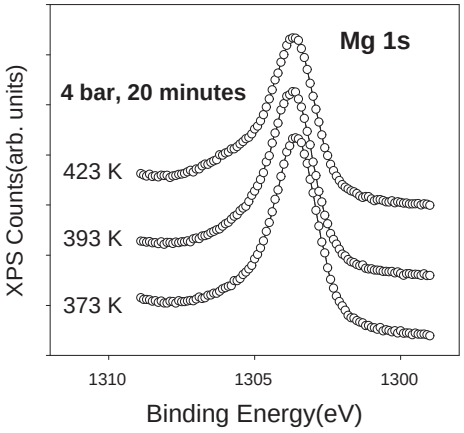

Figure 6.1: XPS spectra of Mg 1s line, obtained after high pressure exposure. hν= 1486.6 eV.

6.2.1 Experimental Details

Prior to use, the high pressure cell was baked in a flow of hydrogen, for 15-24 hours. Given that magnesium has a large affinity for residual water vapour, often present in laboratory gas, the purity of the exposure gas was crucial and could be verified by checking for signs of magnesium oxidation, through measurement of the O 1s photoelectron line with XPS. In order to reduce the possibility of sample contamination, during high pressure hydrogen exposures, the hydrogen was cleaned by passing it over a reduced Cu catalyst, and a molecular sieve. XPS was performed before and after HPC experiments, to check that the magnesium films were indeed oxygen-free. Using the cleaning procedure, it was possible to expose a magnesium film to 40 minutes of 4 bars of hydrogen, without contaminating the surface, as judged from XPS. The thicknesses of the film was chosen such that reproducible results could be obtained, upon exposing the film to high pressures of hydrogen. Ultra-thin films, such as the ones described in Chapter 4, were not compatible with high pressure experiments, as we wanted to be sure that no electronic or structural interactions with the substrate were present. As stated in Chapter 4, a close-packed stacking arrangement is adopted, once the third epitaxial monolayer is completed. However, experiments performed on Mg films of this thicknesses up to 30Å proved to show increased hydrogen dissociation activity. This was presumably due to cracks in the film,

which exposed the substrate. By depositing films with thickness around 400 Å, we obtained reproducible results. Furthermore, we could be certain that the crystal structure of the film was indeed close-packed, thus resembling the structure of bulk magnesium. All HPC experiments reported here were performed in batch-mode.

When performing hydrogen exposures at elevated temperatures, the following procedure was followed.

- Magnesium was evaporated onto the substrate, at 423 K, and the thin film was characterized by XPS.
- The sample was transferred to the high pressure cell, which was sealed off.
- Approximately 100 mbar of hydrogen is leaked into the HPC, in order to verify the quality of the seal, separating the high pressure cell and the analysis chamber. The quality of the HPC seal can be gauged by observing the pressure increase in the analysis chamber.
- If the seal is found to be adequate, i.e. the pressure in the main chamber is below $1{\cdot}10^{-6}$ mbar the HPC is filled to the intended pressure, between 1-4 bars.
- Only after the HPC has reached the desired pressure, is the temperature ramped to desired level.
- When the exposure is finished, the sample heating is interrupted, thus effectively ending the dose, as the temperature plummets down rapidly due to the high thermal conductivity of hydrogen.
- The HPC cell is pumped out with the turbomolecular pump, and the sample is transferred back to analysis chamber, for characterization.

Hydrogen measurement

The hydrogen content in the metallic films can, in principle, be estimated both by means of XPS and TPD. XPS suffers from its inability to probe beyond a few atomic layers. The Mg 1s line, for instance, has an inelastic mean free path of 10 Å, hence information from the bulk is not available. TPD, however, measures the hydrogen content in a destructive fashion. A further advantage of using desorption experiments, is that XPS only provides information about chemical hydride formation, and hence small amounts of atomic hydrogen present as solid solution in magnesium, would be invisible

to the technique. The hydrogen content can also be measured, in real-time, by depositing a magnesium film onto the quartz crystal microbalance, and exposing it to high pressures of hydrogen. In the available setup, no heating of the QCM is possible, and the QCM cannot be transferred to the hydriding cell, thus rendering this option impossible.

Due to the destructive nature of the hydrogen quantification technique, we are able to simultaneously quantify the amount of magnesium deposited, by recording and integrating the m/e=24 signal. Although the magnesium evaporator is frequently calibrated, logging the magnesium signal desorbing, is convenient. While XPS also, to some extent, provides information about the magnesium film thickness, the finite escape depth of the photoelectrons, particularly the Mg 1s line, does not allow for accurate quantification of films with thicknesses around 400 Å.

The hydrogen content is, henceforth, given in units of Mg(0001) monolayers, i.e. $1.94{\cdot}10^{15}$ atoms/cm^2. This is because we wish to be able to relate the hydrogen content to a bulk magnesium coverage for the high pressure experiments, which are performed on thicker magnesium films. The hydrogen saturation coverage defined in Chapter 4, must therefore be rescaled, as it was based on the Mo(111) surface, with a surface density of $5.86{\cdot}10^{14}$ atoms/cm^2. The rescaling factor is therefore $\frac{1.94{\cdot}10^{15}}{5.86{\cdot}10^{14}} = 3.31$.

6.3 Results and Discussion

Figure 6.2 shows the hydrogen and magnesium desorption spectra, after exposing 400Å magnesium films to hydrogen in the high pressure cell. At low hydrogen loadings, the hydrogen desorption curve is very broad, with an almost indistinct peak seen around 500 K. At hydrogen concentrations around 0.6 ML, this peak becomes more pronounced. At loadings above 1, the peak moves upwards, and resembles a zero-order desorption curve. The very sharp peak seen around 600 K at the lowest hydrogen exposure, is due to magnesium desorbing into the mass spectrometer, which prompts a spiking of all the mass spectrometer signals. In order to compensate for an overestimation of the hydrogen signal, a contribution is substracted from the integrated area, of the hydrogen signal.

Figure 6.3 shows the uptake measurements for pure Mg films, obtained at different temperatures. The maximum temperature at which adsorption experiments were performed was 423 K. When attempting experiments at higher temperatures, such as 433 K and 473 K, evidence of magnesium sublimation was seen, in agreement with, for example Fernandez and Sanchez[82], who investigated hydrogen sorption in powders, and also found evaporatory

losses. From Figure 6.3 we see that there is a saturation of the hydrogen uptake, which is temperature dependent. The uptake data are fitted to a second order adsorption isotherm, in order to extract the initial slope of the uptake curve, such that the apparent initial sticking coefficient may be estimated. Due to the quantification technique that we have chosen, the resolution of the hydrogen signal is around 0.5 ML H, which means that an accurate description of the initial hydrogen uptake was not possible.

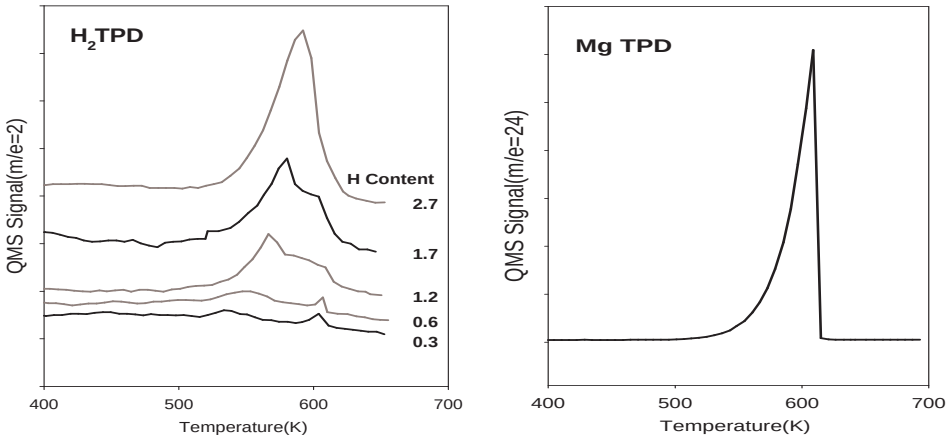

Figure 6.2: On left.Selected hydrogen thermal desorption curves, after 4 bars of hydrogen pressure, at temperatures between 378 and 433 K. On right, Mg TPD for 400Å magnesium film. β= 3 K/s.

On the basis of the apparent initial sticking coefficients, an estimation of the apparent activation energy for dissociative adsorption, ΔE_{act}, can be derived, by plotting the logarithm of the initial sticking coefficient as function of the inverse temperature, due to the relation

$$s(T) = s_0 \exp(\frac{-\Delta E_{act}}{RT}) \tag{6.1}$$

An Arrhenius plot of the initial sticking coefficients is shown in the insert of Figure 6.3. We see that an activation energy of 77.0 kJ/mol is found for hydrogen dissociation, and a prefactor of $5{\cdot}10^{-3}$. This constitutes a sizable discrepancy, compared to the newly published value of the activation barrier, by Vegge[39], who found the barrier to be 110 kJ/mol. The apparent difference can perhaps be explained by the presence of step sites, which have a lower dissociation energy, than terrace sites. This has been seen for several diatomic dissociation reactions. For example, Kratzer and co-workers[83], have studied the dissociation of hydrogen on Si(100) and found step sites to

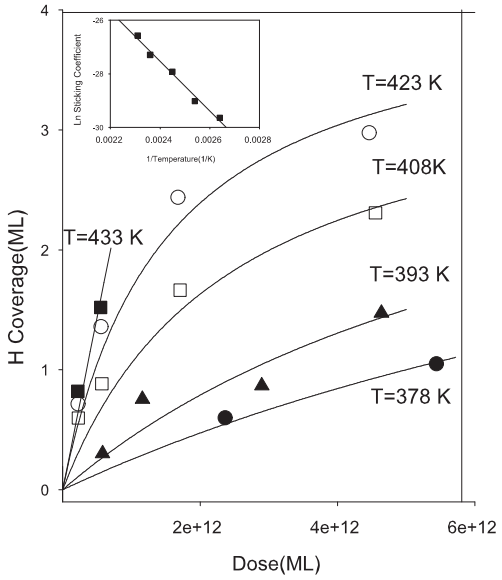

Figure 6.3: The hydrogen coverage, measured with TPD, as a function of H_2 exposure. Solid lines are best fits assuming second order adsorption behavior, and are used to find the initial sticking coefficient, s_o. P(H_2)= 4 bar

be 6 orders of magnitude more reactive, than the corresponding terrace sites, due to a lower barrier for dissociation. Nitrogen dissociation on Ru(0001) has also been shown to be extremely site-specific, with a difference in reactivity of 9 orders of magnitude measured, between step and terrace sites[61], due to differences in activation barriers. We have, in the current undertaking, not investigated the exact structure of the magnesium overlayer, which means that a concentration of step or kink sites cannot be ruled out. Apart from the activation energy, it should be possible to estimate the desorption energy. However, by examining the desorption profile of the most hydrogen-rich film in Figure 6.2, we see that the desorption starts around 550 K. From the magnesium desorption profile also shown, we see that magnesium also begins to sublimate, around this temperature, which renders a desorption analysis difficult. On the basis of the leading edge of the hydrogen desorption curve, we can estimate a desorption barrier around 150 kJ/mol, assuming zero-order desorption.

The fact that the hydrogen uptake, shown in Figure 6.3, is reminiscent of 2nd order adsorption kinetics is not in agreement with the notion that hydrogen diffusion in bulk magnesium, should be fast. Otherwise, a linear

uptake should have been seen. The origin of the transport limitation observed for the magnesium system is not, at the present time, completely clear. However, we believe that it could be due to the formation of an interface hydride, at the vacuum-exposed surface. The formation of an interface hydride has been shown to occur in the Pd/Mg system[50]. These experiments were performed at room temperature, and the H:Mg ratio was between 0.07 and 0.3 for 7800 Å Mg films, i.e. the hydrogen content was much higher than in this work. The authors found that the value of the saturation uptake was inversely proportional to the hydrogen pressure. We did not, in this work, try to vary the hydrogen pressure in order to test of the same were true for the elemental magnesium system. Due to the very low sticking coefficient of hydrogen on magnesium, decreasing the pressure would result in unmanageable exposure times, while increasing the pressure was not compatible with our equipment. Sprunger and Plummer[56] have also found that a metastable hydride phase was formed, upon hydriding a Mg(0001) films with an atomic hydrogen doser.

The observations could also be related to slow diffusion from the surface into the bulk of the film. DFT investigations,by Jacobson and co-workers[40], of the diffusional behaviour of hydrogen in magnesium have shown that the barrier for hydrogen penetration from the surface into the first bulk layer, is much higher than the bulk diffusion value. A barrier for diffusion from the surface into the bulk was found to be around 50 kJ/mol. These investigations are only strictly valid within the low hydrogen concentration, i.e. α-phase. Subsequent diffusion values were found to be in agreement with experimental values, i.e. a barrier around 24 kJ/mol[41].

In Chapter 8, we formulate a model to described hydrogen uptake, which includes rate constants for diffusion, as well as dissociation.

6.4 Conclusions

In this chapter, realistic hydrogen conditions were imposed on a well-defined magnesium film. In agreement with similar investigations of the Pd/Mg system, severe transport limitations were found, at the temperatures and pressures used. Furthermore, it was found that evaporatory losses were found when heating the films to temperatures above 433 K, i.e. the high hydrogen pressure did not appreciably prevent this by the formation of a stagnant gas layer over the film. Finally, it was possible to estimate the dissociative sticking coefficient of hydrogen on magnesium, which, predictably, was found to be quite low. It was scientifically gratifying that the perfect experiment could be carried out, consisting of exposing a clean magnesium surface to high

purity, high pressure gas and forming the hydride phase, without contaminating the surface. However, it was also clear that the perfect experiment could not be unified with the dynamics of a functioning magnesium hydrogen storage system. It should also be remarked, that even though sample handling is crucial, in obtaining oxygen-free magnesium samples, the impurities inherent in laboratory gas will also affect the surface characteristics. Even 1 ppm of water in hydrogen will oxidize the surface completely, at the pressure necessary for uptake.

In Chapter 7, we extend our discussion to include the effect of a catalyst deposited on the surface.

CHAPTER 7

Platinum-promoted Magnesium

This chapter describes the experimental efforts which were aimed at finding novel surface additives, in order to increase the hydrogen dissociation rate. While several past projects[84, 85, 86, 87, 88] have shown that adding a catalytically active material to magnesium aids in promoting hydrogen dissociation, surface characterization has usually been minimal. In this chapter, we use surface analysis, in order to determine the exact composition of the surface of the magnesium film, when promoted with a hydrogen dissociation catalyst.

7.1 Introduction

As can be witnessed from the results presented in the previous chapters, magnesium, on its own, does not seem to work as a feasible hydrogen storage material, in part because of the very low sticking coefficient of hydrogen, found to be around $1{\cdot}10^{-13}$ at 393 K. Apart from the low sticking coefficient, the postulated formation of an interfacial hydride led to a poisoning of the surface, thus limiting hydrogen uptake, at the temperatures where thermal adsorption experiments could be performed. In this chapter, we address the sticking coefficient, by depositing a sub-monolayer coverage of platinum to the surface of well-defined magnesium films.

7.2 Experimental Background

The palladium-magnesium system, discussed in Chapter 2, was useful in assessing the diffusion of atomic hydrogen, as well as the nucleation process of the hydride phase[89]. However, it is quite puzzling that extremely thick palladium films (50Å to 70Å[51]) were necessary in order to obtain hydrogen uptakes, considering that Zaluska and co-workers[32] were able to observe catalytic effects of palladium at loadings around 1 wt%. In the studies of the platinum-magnesium system, presented here, we investigate if the two results can be explained in terms of alloying and segregation phenomena. Furthermore, we extend our discussion to encompass the realistic system involving a coverage of oxygen.

The segregation issue in palladium-magnesium films has been addressed by Krozer and Kasemo[52], who find that at temperatures above 450 K, magnesium segregates to the surface, thus completely covering the catalytic overlayer. The experimental method, by which this was confirmed, was Auger electron spectroscopy, which, due to the finite escape depth of electrons in solids, means that the outermost surface could not be isolated. This is, in itself, in stark contrast to the results presented in [32], where palladium nanoparticles are immobilised at the surface of magnesium particles, during cycling at temperatures above 600 K. TEM pictures, taken before and after hydrogenation, indicated that the palladium nanoparticles were still present at the surface. Gutfleisch and co-workers[48], have investigated the effect of several platinum-group metals, on the hydrogen sorption properties of magnesium-based powders. They observe that high-energy ball-milling results in a nano-crystalline powder, with a lower hydrogen desorption temperature than the correponding microcrystalline powder. Adding platinum or palladium does not further decrease the desorption temperature, which, it is argued, is due to diffusion of the catalyst metal into the bulk of the magnesium particles. It should be remarked that there is some evidence of MgO contamination in the XRD spectra presented in [48].

7.2.1 Experimental details

The experimental procedure used in this chapter is the same as the one used for high pressure exposures of pure magnesium films presented in Chapter 6, with the exception that the pressure read-out in this instance was with a baratron, instead of a pressure controller.

7.3 Results and discussion

7.3.1 Characterization

Initially, the growth of platinum on top of a clean magnesium film was studied, by ISS and XPS, at room temperature. ISS investigations revealed that no platinum was present on the surface. XPS spectra showed, however, that platinum was present, within the escape depth of the Pt 4f line. The deposition rate, obtained by the QCM, also confirmed this. This strongly suggested alloying, even at room temperature. Therefore, we decided to deposit 2 Å platinum on a 400 Å magnesium film, which had been post-oxidized for 400 s, in a partial pressure of $1 \cdot 10^{-7}$ mbar oxygen. Ion scattering investigations of 2 Å platinum deposited on both magnesium and magnesium oxide are shown in Figure 7.1. On the basis of Figure 7.1, it seems clear why segregation phenomena were observed by Gutfleisch and coworkers[48]. Platinum is not, however, stable on the surface of the oxide films, as confirmed by succesive ion scattering investigations at increasing temperatures. At temperatures above 448 K, some evidence of segregation from the surface is seen. We therefore decided to test the hydrogenation behavior of a magnesium film promoted with 0.5 Å Pt, even though ion scattering investigations suggested that the actual surface coverage of platinum was quite low. The platinum coverage was estimated by the rate available to us from the QCM.

7.3.2 Pt-catalyzed Mg

Figure 7.2 shows the results of thermal adsorption experiments, on 400 Å Mg films, promoted with 0.5Å Pt at 1000 mbar H_2, at different temperatures. We clearly see that the uptake is linear, which supports the claim that diffusion away from the interface is fast. Remarkably, no blocking of the surface due to the formation of a surface hydride, was seen, unlike the results of thermal adsorption on pure magnesium films. No experiments were carried out in an attempt at mapping out the optimal or minimum platinum coverage for hydrogen dissociation. Figure 7.3 shows the thermal desorption spectra of hydrogen from Pt-catalyzed magnesium films. No signs of molecular hydride, MgH_2, desorption could be observed, as measured by the m/e=26 signal in the mass spectrometer. At increasing hydrogen coverages, the desorption peak shifts upwards, implying self-stabilization of the hydride phase. This behaviour was, in fact, also observed in Chapter 4, for magnesium hydride films formed by means of an atomic hydrogen doser. The fact that platinum strongly segregates into the bulk of the material was confirmed by depositing platinum at 423 K, and annealing for 10 minutes. Subsequent high pressure

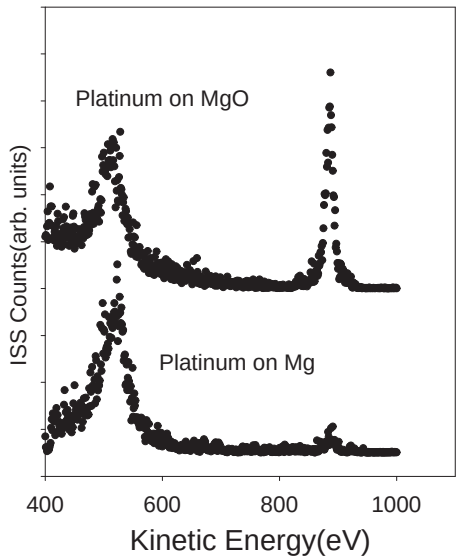

Figure 7.1: He^+ ion scattering spectra. 2 Å platinum deposited on 400 Å magnesium and magnesium oxide films, respectively. ¡The magnesium oxide film was formed by post-oxidizing a metallic 400 Å Mg film for 400s, in $1{\cdot}10^{-7}$ mbar.

experiments indicated a substantial decrease in hydrogen sorption, as shown in Figure 7.2.

The sticking coefficient, as obtained from the slope of the uptake curves in Figure 7.2 is shown in Figure 7.4, as function of reciprocal temperature. Also shown in the plot are the data points from hydrogen sticking on non-catalyzed magnesium, described in Chapter 6. We see a drastic increase in the sticking coefficient. Single hydrogenation experiments for the Pt-catalyzed system were also attempted at temperatures above 348 K, and are shown as open triangles. Due to the availability of only a single hydrogen exposure at these temperatures, these data points were not included in the estimation of the activation barrier. We see, however, that they are in general agreement with the rest of the data. When comparing the sticking coefficients, we find that the sticking probability is increased by a factor of 12000, at room temperature. However, care must be exercised when interpreting that number, as the platinum coverage is actually below the detection limit of ion scattering spectroscopy, which means that nominal difference in sticking coefficient could be 2 orders of magnitude higher.

Figure 7.5 shows the thermal desorption of 3 ML of hydrogen, from a

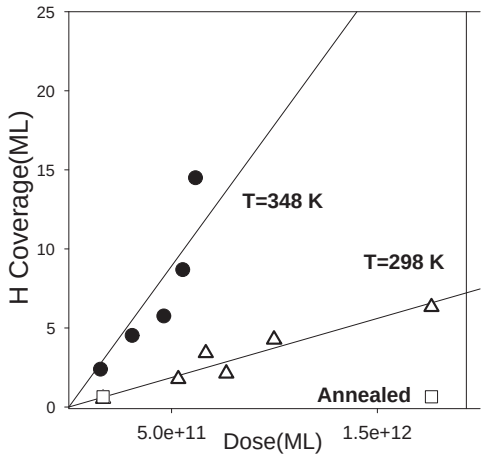

Figure 7.2: Hydrogen uptake, at different temperatures, for 400 Å Mg/0.5Å Pt system. P(H_2=1000 mbar.) Lines shown are linear fits to uptake data.△: T= 298 K. •: T=348 K. □: Annealed to 423 K, prior to high pressure exposure at 298 K.

400 Å magnesium film, and from a Pt-promoted 400 Å Mg film. We see that there is no change in the desorption temperature, or shape of the profile. This suggests that the platinum overlayer does not influence the desorption profile of hydrogen in magnesium hydride.

7.3.3 The effect of oxygen

From Figure 7.1, it is clear that at room temperature, a partial overlayer of platinum is not stable on a magnesium surface, due to alloying. It was, however, remarkable, that a drastic increase in the dissociative sticking coefficient of hydrogen was seen anyway. The introduction of oxygen as an impurity, stabilized platinum at the surface as observed with low-energy ion scattering. The hydrogenation properties of Pt-catalyzed magnesium films, precovered with oxygen, were therefore studied.

A number of different hydrogen adsorption experiments were conducted, to illuminate the combined effect of a hydrogen dissociation catalyst, and different overlayers of magnesium oxide. These are listed.

A: 0.5Å Pt deposited on top of a 400 Å Mg film. This experiment addresses the effect of the platinum catalyst on hydrogen uptake.

B: 0.5 Å Pt deposited on top of a 400 Å Mg film, which has been exposed to $5 \cdot 10^{-7}$ mbar O_2 for 1000 s. This experiment addresses the mobility

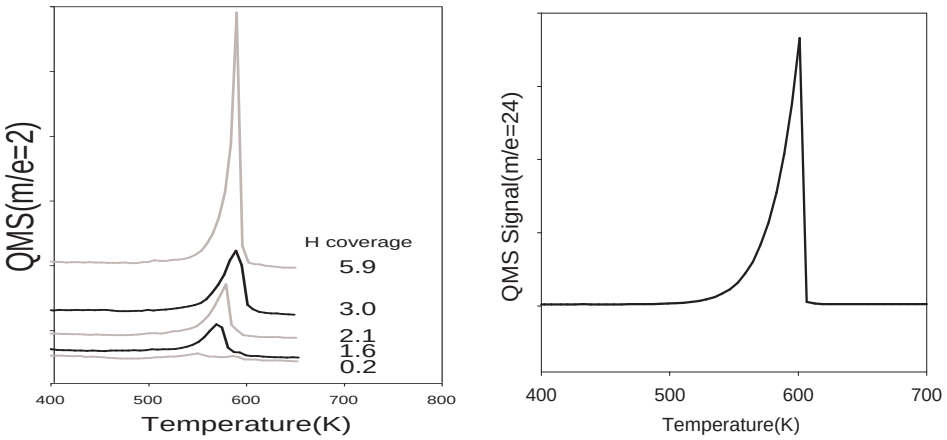

Figure 7.3: On left.Hydrogen desorption curves, for 400 Å Mg film, promoted with 0.5 Å Pt. β=3 K/s. On right, Mg TPD for 400 Å magnesium film, promoted with 0.5 Å Pt β= 3 K/s.

of atomic hydrogen through a magnesium oxide phase, which has been formed by post-oxidation.

C: 0.5 Å Pt deposited on top of a 400 Å Mg film, which has been covered by a stoichiometric MgO overlayer of thickness 10 Å. This experiment adresses the mobility of atomic hydrogen, through a magnesium oxide phase, which has been formed by simultaneous dosing of magnesium and oxygen, and thus is highly stoichiometric.

D: 0.5 Å Pt deposited on a 400 Å Mg film, which is subsequently exposed to $1{\cdot}10^{-8}$ mbar O_2, for 100 s. This experiment investigates whether or not the hydrogen dissociation catalyst stays on the surface of a magnesium film, upon oxidation.

E: 400 Å Mg film, oxidized in $1.5 \cdot 10^{-8}$ mbar, for 60 s. In this experiment, we see if hydrogen dissociation is promoted by the presence of partial overlayer of magnesium oxide. Density functional theory predicts a higher barrier than on pure magnesium[90].

The hydrogen uptake, as determined by thermal desorption of hydrogen are shown in Figure 7.6. We see that the MgO films formed by post-oxidation, shown in Figure 7.6 B, do not form a complete diffusion barrier for hydrogen dissociated at the surface, although a slight reduction in the uptake is seen. A 10 Å MgO film formed directly, by evaporating magnesium in an oxygen back-pressure, does not allow atomic hydrogen passage,

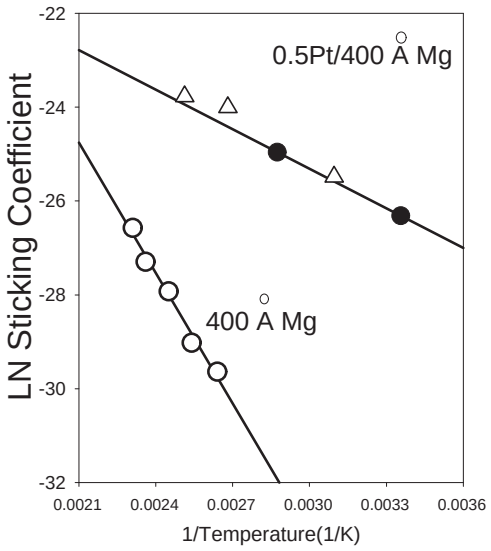

Figure 7.4: Sticking coefficient, obtained by thermal adsorption experiments. An activation energy of 23 kJ/mol is found for Pt-promoted Mg films.○: Pure Mg. •: 0.5Å Pt/400Å Mg. △. 0.5Å Pt/400Å

in agreement with Gonzalez and co-workers, who studied diffusion in MgO crystals[35]. We furthermore see that the Pt catalyst segregates from the surface, upon surface oxidation, shown in Figure 7.6D. Finally, the control experiment, showed a remarkably reduced uptake rate.

The results of these investigations, concerning magnesium as a hydrogen storage material, promoted with platinum, clearly show that hydrogen dissociation can be enhanced substantially, by the deposition of a fractional monolayer of a catalytically active metal. The mobility of the hydrogen dissociation catalyst was shown to be substantial even at temperatures around 423 K. We managed to show, however, that platinum could be somewhat immobilized on oxidized magnesium layers.

An oxide overlayer seems, in our opinion, to offer a possible solution for catalyst immobilisation. In Chapter 5, we also argued that magnesium oxide also exerted a stabilizing effect, thus preventing magnesium sublimation. It is, finally, interesting to note that hydrogen diffusivity through post-oxidized Mg films was finite even at room temperature. This has also been observed in the work of Hjort and co-workers[73], who found measurable hydrogen sorption rates even through heavily oxidized magnesium films[1].

[1] A single experiment, consisting of oxidizing a magnesium film in 0.13 mbar O_2 also

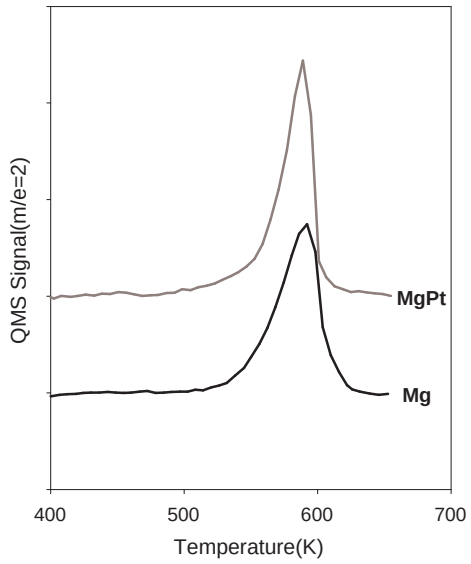

Figure 7.5: Thermal desorption of approximately 3 ML H, for 400 Å magnesium, and for 400 Å Mg promoted with with 0.5 Å Pt. β= 3 K/s

If we extend the discussion to encompass powder-based systems, it could be speculated that much of the published literature concerning catalyzed magnesium powders, in fact contains a partial coverage of magnesium oxide, which serves as both a structural binder, which prevents magnesium sublimation, and doubles as an anchoring point for the hydrogen dissociation catalyst.

As for hydrogen adsorption in the catalyzed and non-catalyzed magnesium samples, we noted completely differing uptake behaviour in the two different cases. For platinum-catalyzed magnesium films, the uptake was linear, at least up to the hydrogen loadings which were investigated, while the pure magnesium system showed a clear indication of stagnation in the uptake. These two results are seemingly incongruent, as the effect of the partial overlayer of platinum should only be related to an enhancement of the dissociation kinetics. However, it is likely that the introduction of platinum to the surface, results in the formation of a Mg-Pt surface alloy, whereby the surface hydride formation is prevented.

resulted in measurable hydrogen uptake rates.

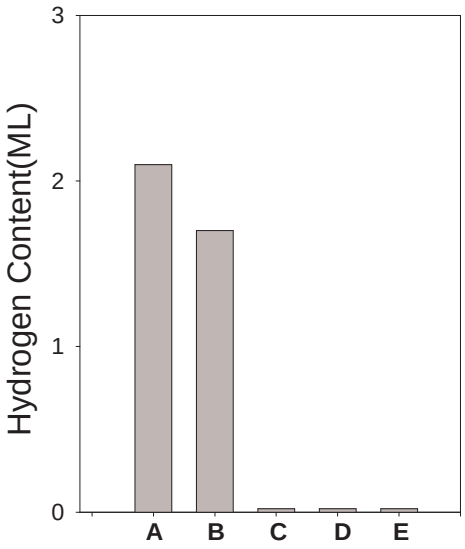

Figure 7.6: Amount of hydrogen adsorbed for Pt/MgO/Mg system. Hydrogen exposure was 4.5-6·10^{11} ML, at room temperature. P(H_2)=1000 - 1800 mbar. **A**: 0.5 Å Pt/ 400 Å Mg. **B**: 0.5 Å Pt/MgO_x /400Å Mg. **C**: 0.5 Å Pt/ 10Å MgO/ 400Å Mg. **D**: MgO_x/0.5Å Pt/400 Å Mg. **E**: MgO_x/400Å Mg. For a description of the oxidation procedure, please refer to page 69.

7.4 Conclusions

Using a combination of standard surface science tools, along with the high pressure cell, we have established the following:

- Magnesium and platinum alloy readily at room temperature, as observed by ion scattering investigations.
- The dissociative sticking probability increases by more than 4 orders of magnitude, at room temperature, upon adding a partial monolayer of platinum to the surface.
- A linear uptake of hydrogen was found, upon promoting 400 Å magnesium films with 0.5 Å Pt.
- Platinum can be immobilised at the surface at room temperature, by introducing oxygen as an impurity. Atomic hydrogen is seen to diffuse through post-oxidized magnesium oxide films. Atomic hydrogen

diffusion through stoichiometric magnesium oxide overlayers was immeasurably slow.

The fact that ion-scattering investigations of the platinum-promoted magnesium film in fact suggested that no measurable amount of platinum was present at the outermost surface, sets this work apart from the similar undertakings carried out on the palladium-magnesium system, where the catalyst overlayer was 60-70 Å thick, and underlines how poorly magnesium dissociates hydrogen.

CHAPTER 8

Modelling Hydrogen uptake

This chapter covers a numerical approach to describing the uptake of hydrogen in magnesium.

8.1 Introduction

In Chapter 2, the hydrogen sorption process was described as being comprised of a number of steps, occurring in succession. In this chapter, we introduce a strongly simplified model, which models the hydrogen uptake, by adressing each of the elementary steps, and setting up rate equations for each.

Several approaches to modelling hydrogen uptake in magnesium have been previously seen in the hydrogen storage literature. Spatz et. al[43], for example, have studied hydrogen uptake in palladium-covered magnesium films, and by relating the chemical shift of the Mg 1s photoelectron line to the temporal evolution of the extent of hydride formation, a model was proposed from where an overall diffusion coefficient was derived. However, from the experimental data presented, the hydride saturation content could not, in general, be related to the magnesium film thickness. The effect of temperature was also not studied. Zhdanov and co-workers[89] described a model where it was assumed that the irreversible hydride nucleation was the result of hydrogen atoms colliding. The model was, in turn, related to experimental findings describing hydrogen uptake in palladium-covered magnesium films, where a qualitative agreement was found. These two models did not adress the issue of dissociative sticking of hydrogen, due to the presence of the

palladium overlayer.

The hydrogenation of a metal like magnesium consists of a number of successive events. These events include H_2 transport to the surface, diffusion to the active (bridge) site[37, 38, 39], hydrogen dissociation, diffusion into subsurface, bulk diffusion, followed by β-phase nucleation. The main difficulty in defining a model which models the overall uptake is obtaining values for the activation barriers for each of the steps. An experimental value, of 24 kJ/mol, for the activation barrier for diffusion of atomic hydrogen in magnesium has been obtained by Nishimura and co-workers[41]. An activation energy around 100 kJ/mol for the diffusion of hydrogen through β-MgH_2 has been found by Fernandez and Sanchez[82].

Vegge[39] recently calculated a number of these and other values[1] for low hydrogen concentrations, i.e. solid solution of hydrogen in magnesium, by using a first-principles calculational approach, based on density functional theory. As the magnesium surface was modelled using 20 Mg atoms, the issue of hydride blocking was not addressed, i.e. a diffusion constant which was coverage dependent. Jacobson and co-workers[40], have also studied the diffusion properties of hydrogen on Mg(0001), and found a barrier of 48 kJ/mol, for diffusion from the surface into the bulk, thus suggesting a possible rate-limiting step involving the transport of hydrogen from the surface layer. Up to now, a model has not been proposed which, on one hand addresses each individual step in the hydride formation process, and on the other hand can be related to experiments performed under controlled, yet realistic conditions.

In this chapter, a general model is proposed which incorporates values for the activation energies of the different steps, obtained from experimental and theoretical data. As will be evident, the model captures, within reason, the sorption rates measured under laboratory conditions, for the simplest hydrogen storage system studied.

8.2 Model

A number of rate equations are set up describing the following atomic concentrations.

- Surface layer: Contains contributions from dissociative sticking, molecular desorption, and diffusion in and out of bulk. We assume that the maximum coverage of the surface is 1.

[1] Other sorption related events calculated by Vegge included barriers for hydrogen mobility on the Mg(0001) surface as well as diffusion into the first magnesium layer.

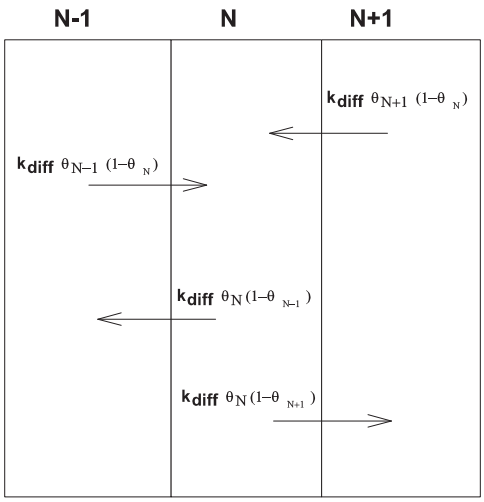

Figure 8.1: Schematic illustration of hydrogen transport in Nth atomic layer of magnesium, as defined in the model.

- First bulk layer: Contains diffusion contributions from the surface and bulk. We assume that the maximum coverage of the subsequent bulk layers is 2, in order to allow for stoichiometric MgH_2 formation.
- Rest of bulk layers θ_N: Contains diffusion contributions to and from neighboring layers
- Last layer $\theta_{N_{max}}$: Boundary condition, i.e. no transport through last layer.

The change in coverage in the surface layer, θ_S can be written as

$$\frac{d\theta_s}{dt} = \frac{2S_0F\exp(-E_A/kT)}{N_s}(1-\theta_s)^2 - \nu_{des}\exp(-E_{des}/kT)\theta_s^2 - \nu_{sb}\exp(-E_{sb}/kT)\theta_s(2-\theta_1) + \nu_{bs}\exp(-E_{bs}/kT)\theta_1(1-\theta_s)$$

The symbols are defined in Table 8.1. Similarly for the first bulk layer, the change in coverage can be written as.

$$\frac{d\theta_1}{dt} = \nu_{sb}\exp(-E_{sb}/kT)(2-\theta_1)\theta_s + \nu_d\exp(-E_d/kT)(2-\theta_1)\theta_2 - \nu_{bs}\exp(-E_{bs}/kT)(1-\theta_s)\theta_1 - \nu_d\exp(-E_d/kT)(2-\theta_2)\theta_1$$

In order to generalize the equation for an arbitrary film thickness, an index, N, is introduced, describing the subsequent individual layers in the bulk of

the film. Figure 8.1 shows the hydrogen transport to and from the Nth layer.

$$\frac{d\theta_N}{dt} = \nu_d \exp(-E_d/kT)(2-\theta_N)(\theta_{N-1}) + \nu_d \exp(-E_d/kT)(2-\theta_N)\theta_{N+1} - \nu_d \exp(-E_d/kT)(2-\theta_{N+1})\theta_N - \nu_d \exp(-E_d/kT)(2-\theta_{N-1})\theta_N$$

A boundary condition is introduced such that the rate of change in the last layer, N_{max}, can be written as

$$\frac{\theta_{N_{max}}}{dt} = \nu_d \exp(-E_d/kT)(2-\theta_{N_{max-1}})\theta_{N_{max}} - \nu_d \exp(-E_d/kT)(2-\theta_{N_{max}})\theta_{N_{max-1}}$$

i.e., no hydrogen transport beyond the last layer.

As an initial approximation, we assume that the hydrogen diffusion in bulk magnesium is coverage independent. The diffusion coefficient has been determined experimentally by Nishimura and co-workers,[41], who find an activation energy of 24 kJ/mol. The prefactor, ν, can be estimated through the relation[92]

$$D_0 = h\nu\lambda^2 \tag{8.1}$$

where h is a geometrical constant of the order of unity, D_0 is the experimentally determined prefactor for hydrogen diffusing in magnesium, 1.54 x $10^{-6} m^2/s$ and λ is the jump distance. On the basis of this relation, we find that a prefactor of the order of $10^{13} 1/s$ is a sound assumption.

Table 8.1 summarizes the values used in the solution of the system of differential equations.

8.3 Modelling Results

8.3.1 H Solution: α-phase

The α-phase of magnesium represents the amount of hydrogen which can be present as solid solution. The heat of solution is endothermic, around 21-24 kJ/mol[91]. The amount of hydrogen, x_H, bound as α-phase is a function of temperature, T, and is given as[91]:

$$ln(x_H) = 4.67 - \frac{6225}{T} \tag{8.2}$$

We see that at T=423 K, the hydrogen content, x_H is $4.3 \cdot 10^{-5}$. This indicates that the hydrogen present as solid solution cannot explain the hydrogen desorption spectra seen in Chapter 6.

Symbol	Physical constant	Value	Unit
N_s	Surface density	1.94 x10^{19}	$1/m^2$
ν_d	Prefactor:Bulk Diffusion	10^{13}	1/s
ν_{des}	Prefactor:Desorption	10^{13}	1/s
ν_{bs}	Prefactor:Bulk-tosurface diffusion	10^{13}	1/s
ν_{sb}	Prefactor:Surface-to-bulk diffusion	10^{13}	1/s
E_{des}	Desorption barrier	151.5	kJ/mol
E_A	H_2 dissociation barrier	77	kJ/mol
E_d	Diffusion barrier	24	kJ/mol
S_0	Initial sticking prefactor	$5{\cdot}10^{-3}$	-
E_{bs}	Bulk to surface diffusion barrier	24	kJ/mol
E_{sb}	Surface to bulk diffusion barrier	24	kJ/mol
Δ H	Enthalpy of formation: MgH_2	74.5	kJ/mol
N_{max}	Number of slabs	100	-

Table 8.1: Numerical values used for solving uptake equations

8.3.2 Hydride formation

The hydride formation process is highly exothermic. ΔH for this process is -74.5 kJ/mol[23]. This has a natural consequence when dehydriding magnesium hydride, as a large amount of heat must be continuously supplied. A general source of scrutiny, regarding the hydriding process, is that the formation of hydride grains can serve as hydrogen diffusion blockers. The activation energy for hydrogen diffusion through rutile β-MgH_2 has recently been studied by Oskarsson and co-workers[93]. Here, they find that, the barrier is above 200 kJ/mol, due to the high energy cost associated with forming a vacancy in the rutile structure. This is offered a possible explanation for sluggish hydriding kinetics. The formation of rutile MgH_2 can be included in the model by assuming a diffusional activation energy in between 20 kJ/mol and 200 kJ/mol. Figure 8.2 shows the energy diagram for MgH_2 formation. A variation in the diffusional activation energy can be included through an increase in E_d.

Figures 8.3 shows the results of hydrogen uptakes, at various temperatures, with different diffusional activation energies. We see that if we assume an activation energy of 24 kJ/mol, as predicted by experiment and theory, the total hydrogen uptake is not linear. By examining the hydrogen content of the individual magnesium slabs, shown in Figure 8.4, we see that the concentration in each bulk layer is the same, when E_d= 24 kJ/mol. Therefore, the stagnant uptake is due to site-blocking on the surface, thus limiting hy-

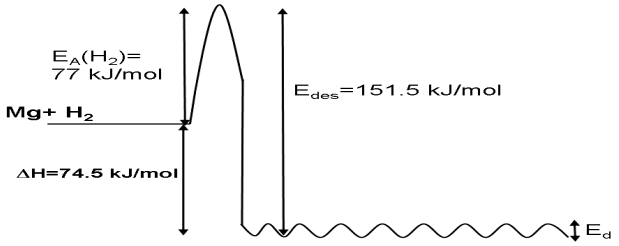

Figure 8.2: Schematic illustration of the exothermic hydride formation. Δ H is the heat of formation of the hydride phase, $E_A(H_2)$ is the activation barrier for hydrogen dissociation, E_d is the bulk diffusion barrier for hydrogen in magnesium, and E_{des} is the desorption energy.

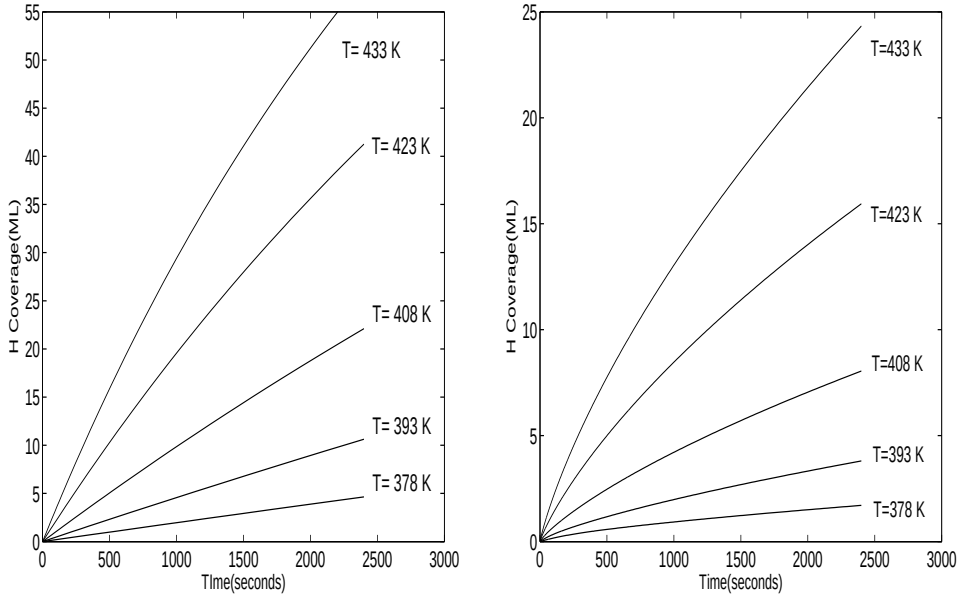

Figure 8.3: Effect of diffusional activation energy on overall hydrogen uptake, $\sum_{n=1}^{N_{max}} \theta_n$ at various temperatures. P(H_2)=4 bar. Left panel, E_d=24 kJ/mol. Right Panel E_d=120 kJ/mol.

drogen dissociation. If the diffusional activation energy is increased to 120 kJ/mol, in order to mimick the effect of hydride build-up, we note a different behaviour. Apart from the decrease in the total hydrogen uptake, shown in Figure 8.3, we see that the concentration in the individual slabs are no longer "in phase", thus forming a gradient through the film. The value at which

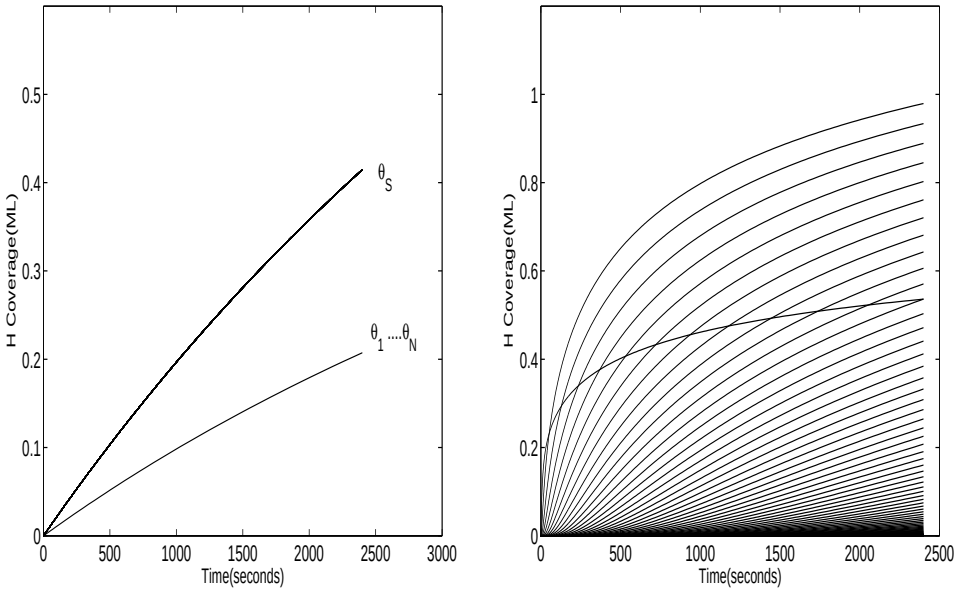

Figure 8.4: Effect of diffusional activation energy hydrogen uptake, in individual slabs, at 423 K. P(H_2)=4bar. Left panel, E_d=24 kJ/mol. Right Panel E_d=120 kJ/mol.

the system switches from being diffusion-controlled to sticking-controlled is found to be E_d= 80 kJ/mol, at T= 423 K. At higher temperatures, this value increases. If we assume an operating temperature of 600 K, the value of the diffusion barrier increases to 140 kJ/mol, below which dissociative sticking is rate-determining. In our experimental section, it was, of course, not possible to perform hydrogenation experiments at this temperature.

Finally, the thermal desorption of hydrogen was simulated, on the basis of the energy diagram in Figure 8.2. This is shown in Figure 8.5. We naturally observe 2nd order desorption behaviour, but note that the maximum desorption rate occurs at temperatures above 600 K, which is above the temperature at which hydrogen desorption was seen for the catalyzed and non-catalyzed magnesium films. At this temperature, the evaporation rate of magnesium is around 100 ML/second, which suggests that the model does not accurately depict the observed features, presented in Chapters 6 and 7.

8.3.3 Comparison to experiment

In Chapter 6, we presented data which described the hydrogen uptake on well-defined magnesium films. It was clear that hydrogen transport into the

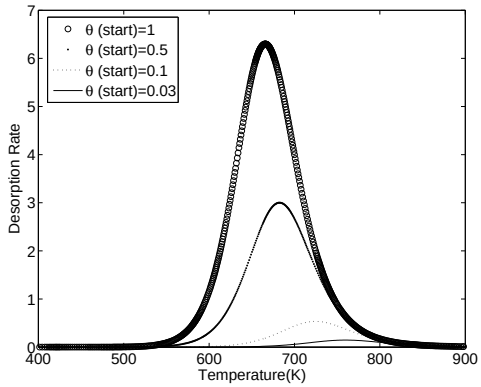

Figure 8.5: Simulated thermal desorption of hydrogen, for magnesium films with different hydrogen contents.$\theta(start)$ denotes the hydrogen content. Based on energy diagram from Figure 8.2

bulk saturated at a low value, with a total hydrogen uptake of only 3 ML realized at 423 K. We speculated that the stagnant uptake perhaps could be related to the formation of an interfacial hydride, which prevented further hydriding. To model the formation of an interfacial hydride, an energy diagram was adapted, shown in Figure 8.6, where a deep trough was introduced immediately following dissociation. Thereby it follows that the barrier for penetration into the bulk increases, as well, in agreement with theoretical low-coverage hydrogen diffusion calculations[39, 40].

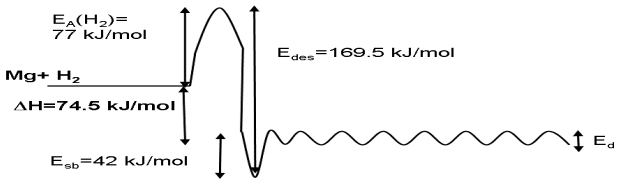

Figure 8.6: Energy diagram of hydride formation, with interfacial hydride included. E_{sb}= 42 kJ/mol

Figure 8.7 shows the results of the simulated hydrogen uptakes. We immediately see the introduction of a surface state reduces the total hydrogen uptake by a factor of 20, relative to the results shown in Figure 8.3. In Figure 8.7, the hydrogen uptake data from Chapter 6 are included. The fitting

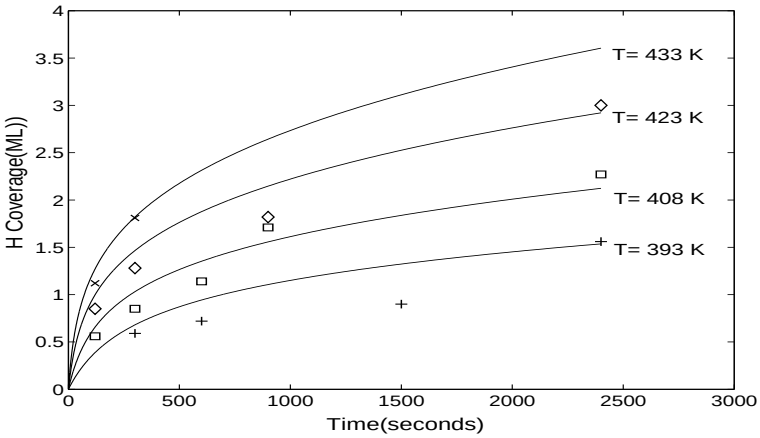

Figure 8.7: Simulated hydrogen uptake curves, based on energy diagram in Figure 8.6. P(H_2)= 4 bar.Experimental data assigned the following symbols. +: T= 393 K. □: T= 408 K. ◇: T= 423 K. ×: T= 433 K

parameter used in this instance was the value of the activation barrier for diffusion from the surface state into the bulk. The best fit was found for E_{sb}=42 kJ/mol, which corresponds to an increase of 18 kJ/mol relative to the barrier for bulk diffusion. This, in turn, influences the value of the desorption barrier, which is also increased by 18 kJ/mol. It could be argued that there are some qualitative similarities, but no perfect agreement is found. In particular, the saturation value, obtained after 40 minutes exposure, seems to be in agreement with the model.

It was not possible to accurately model the thermal desorption of hydrogen from the magnesium surface. This, we believe, is due to the sublimation of magnesium occurring at moderate temperatures. The model described here does not take this into account, which explains the observed discreprancy.

The advantage of the model is that the complexity can be increased, by, for example, including coverage dependent energy barriers, such as diffusion barriers. Furthermore, the kinetics of isothermal hydrogen release can be studied through proper choice of initial conditions. This was not pursued as the experimental data available to us was limited.

8.4 Conclusions

By combining theoretical and experimental values for the various stages of the hydrogen sorption process, a model was developed based on a planar geometry, to model hydrogen uptake in metal films of arbitrary thickness. It was described how large the diffusional activation energy has to be in order for diffusion to become rate-controlling, under the given temperatures and pressures used. By comparing the results of the model with hydrogen uptake curves obtained under controlled conditions, some qualitative agreement is found. We were also able to suggest an explanation in the apparent hydrogen transport limitation, through the introduction of a surface hydride state. It should be noted that other experimental findings established that the limiting hydride state was meta-stable, and vanished at 425 K, which suggests that at higher temperatures, hydrogen transport should not present a problem[56].

CHAPTER 9

Conclusions and Outlook

In the work presented here, the Mg-based hydride system has been investigated in some detail. Using a combination of standard surface science techniques, and a high pressure cell, we have demystified the system to some extent. Amongst other things, we have established the following:

- When depositing ultra-thin magnesium films, up to a few monolayers, onto a hydrogen-covered molybdenum substrate, an adsorbed overlayer of hydrogen is found to be stable, the structure of which was confirmed by density functional calculations
- When forming a hydride with an atomic hydrogen doser, hydrogen release is only observed when magnesium is evaporating, during the course of desorption experiments.
- The apparent activation barrier for hydrogen dissociation on magnesium was found to be 77 kJ/mol, and the sticking coefficient is $1{\cdot}10^{-13}$ at 393 K.
- The activation barrier for hydrogen dissociation can be reduced to 23 kJ/mol through the addition of platinum to the surface.
- Magnesium oxide serves as a structural stabilizer for magnesium, without which extreme loss of surface area would be sustained in a nanoparticle scenario.
- A model was sketched out, which, appeared to capture some features of hydrogen uptake in pure magnesium films. While some assumptions

were made, in order that the experimental data could be modelled, the generality of the model makes it applicable in a wider framework.

A major conclusion, which can be drawn from the work, is that the model system approach was able to clearly illustrate that the simple perception of hydride formation cannot explain the workings of a state-of-the-art hydrogen storage rig. By, in steps, increasing the complexity of the model system, some continuity could be established, which could be projected onto the real system.

Due to the rapid evaporation rates observed, for impurity-free magnesium films, a proper analysis of the hydrogen desorption behaviour could not be performed. The hydrogen desorption could, however, be used as a convenient hydrogen quantification technique. This way, we were able to obtain some quantitative data, concerning the barriers for hydrogen dissociation, on promoted and non-promoted magnesium.

The key to understanding this material fully involves the full comprehension of the role of magnesium oxide. In the experimental work, it was suggested that oxide impurities help to stabilize the magnesium particles, while, at the same time, were permeable to atomic hydrogen diffusion. The paradox about this material is that while substantial efforts, were exerted in order to prevent oxide contamination, in the end, the oxide was a necessity in the model system.

As for the contribution of this work to the hydrogen storage literature, I believe that since it was possible, to assess and evaluate the oxygen content directly, a novel way of understanding the material has opened up. Instead of treating magnesium-hydride as a bi-component system, serious thought should be given to the increased understanding of the oxide component, particularly the details of hydrogen permeation and activation. I also believe that catalyst mobility is important, and our ability to essentially anchor the catalyst on the surface represents an important feature to be addressed in attempt at engineering a better magnesium-based storage medium.

BIBLIOGRAPHY

[1] Chorkendorff, I., and Niemansverdriet, H. *Concepts of Modern Catalysis and Kinetics*. WILEY-VCH. 2003

[2] Ogden, J., Annual Review of Energy and the Environment. 227(1999)

[3] http://www.wtrg.com

[4] *Hydrogen Posture Plan. United States Department of Energy*. February 2004

[5] Linsebigler, A.L., Lu, G., Yates, J.T. Chemical Reviews. **95**. 735(1995)

[6] Gratzel, M. Nature. **414**. 338(2001)

[7] Steele, B.C.H., and Heinzel, A. Nature. **414**. 345(2001)

[8] Smith, A. and Linderoth, S. Teknisk Nyt nr. 5(DANISH). 30(2005)

[9] Ormerod, R.M. Chemical Society Reviews. **32**. 17(2003)

[10] Carden, P.O., and Paterson L. International Journal of Hydrogen Energy. **4**. 559(1979)

[11] Irani, R.S. MRS Bulletin. **September**. 680(2002)

[12] Wolf, J., MRS Bulletin. **September**.684(2002)

[13] Berry, G.D, and Aceves, S.M. Energy and Fuels. **12**. 49(1998)

[14] Schlapbach, L.,Züttel, A. Nature. **414**. 353(2001)

[15] Chambers, A., Park, C., Baker, R. T. K., Rodriquez, N.M. Journal of Physical Chemistry B. **102**. 4253(1998)

[16] Liu, C., Fan, Y.Y.,Liu, M., Cong, H.T. Cheng, Dresselhaus, M.S., H.M. Science. **286**. 1127(1999)

[17] Chen, P.,Wu, X., Lin, J., Tan, K.L. Science. **285**. 91(1999)

[18] Yang, R.T. Carbon. **38**. 623(2000)

[19] Zandonella, C. Nature. **410**. 734(2001)

[20] Guay, P.,Stansfield, B.L., Rocheforst, A. Carbon. **42**. 2187(2004)

[21] Schuth, F., Bogdanovic, B., Felderhoff, M. Chemical Communications. 2249(2004)

[22] Westlake, D.G. Journal of the Less-Common Metals. **91**. 275(1983)

[23] Sandia National Laboratories. *Hydride Information Center.* http://hydpark.ca.sandia.gov/

[24] Bogdanovic, B. and Schwikardi, M.J. Journal of Alloys and Compounds. **253**. 1(1997)

[25] Luo, W. and Gross, K.J. Journal of Alloys and Compounds. **385**. 224(2004)

[26] Gross, K.J., Majzoub, E.H., Spangler, S.W. Journal of Alloys and Compounds. **356-357**.423(2003)

[27] Wang, P., and Jensen C.M. Journal of Alloys and Compounds. **379**. 99(2004)

[28] Walters, R.T. and Scogin, J.H. Journal of Alloys and Compounds. **379**. 135(2004)

[29] Gross, K.J., Guthrie, S., Takara, S., Thomas, G. Journal of Alloys and Compounds. **297**. 270(2000)

[30] http://www.bgs.ac.uk/mineralsuk/home.html. *British Geological Survey*

[31] Vigeholm, B. Chemical Energy Storage Based on Metal Hydrides; Technical Report Risø-M-2608, Risoe National Laboratory, DK-4000 Roskilde, Denmark, 1989 (In Danish).

[32] Zaluska, A., Zaluski, L., Strom-Olsen, J.O. Journal of Alloys and Compounds. **288**. 217(1999)

[33] Zaluski, L., Zaluska, A., Tessier, P., Strom-Olsen, J.O., Schulz, R. Journal of Alloys and Compounds. **217**. 295(1995)

[34] Fournier, V., Marcus. P., Olefjord,. I. Surface and Interface Analysis. **34**. 494(2002)

[35] Gonzalez, R., Chen, Y., Tsang, K.L. Physical Review B. **28**. 4637(1982)

[36] Chen, C.P., Liu, B.., Li, Z.P., Wu, J., and Wang, Q., D. Zeitschrift fur Physikalisches Chemie. **181**. 259(1993)

[37] Bird, D.M., Clarke, L.J., Payne, M.C., Stich, I. Chemical Physics Letters. **212**. 518(1993)

[38] Nørskov, J.K., Houmøller, A., Johansson, P.K., and Lundqvist. Physical Review Letters.**46**. 257(1981)

[39] Vegge, T. Physical Review B. **70**. 35412(2004)

[40] Jacobson, N.,Tegner, B.,Schroder, E., Hyldgaard, P.,Lundqvist, B.I. Computational Materials Science. **24**. 273(2002)

[41] Nishimura, C. Komaki, M., Amano, M. Journal of Alloys and Compounds. **293-295**. 329(1999)

[42] Renner, J. and Grabke, H.J. Zeitscrift fur Metallkunde. **69**. 639(1978)

[43] Spatz, P., Aebischer, H.A., Krozer, A., Schlpapbach, L. Zeitschrift fur Physikalisches Chemie. **181**. 393(1993)

[44] Gross, K.J. PhD Thesis. Fribourg, Switzerland. 1999.

[45] Rudman, P.S. Journal of the Less-common Metals. **89**. 93(1983)

[46] Huot, J., Liang, G., Schulz, R. Applied Physics A. **72**. 187(2001)

[47] Andreasen, A., Vegge, T., and Schroder-Pedersen, A. Journal of Physical Chemistry B. **109**. 3340(2005)

[48] Gutfleisch, O, Schlorke-de Boer, N.,Ismail, N.,Herrich, M., Walton A.,Speight, J., Harris, I.R., Pratt, A.S., Zuttel, A. Journal of Alloys and Compounds. 356-357(2003). 598(2003)

[49] Herrich, M., N. Ismail, N., Lyubina, J., Handstein, A., Pratt, A., and Gutfleisch O. Materials Science and Engineering. **B108**. 28(2004)

[50] Krozer, A. and Kasemo, B. Journal of Vacuum and Science Technology. **5**. 1003(1986)

[51] Hjort, P., Krozer, A., Kasemo, B. Journal of Alloys and Compounds. **234**. L11(1996).

[52] Krozer, A and Kasemo, B. Journal of the Less-common Metals. **160**. 323(1990)

[53] Yoshimura, K., Yamada, Y., Okada, M. Surface Science. **566-568**. 751(2002)

[54] Higuchi, K., Kajioka, H., Toiyama, K., Fujii, H., Orimo, S., Kikuchi, Y., Journal of Alloys and Compounds. **293-295**, 484(1999)

[55] Higuchi, K., Yamamoto, K., Kajioka, H., Toiyama, K., Honda, M., Orimo, S., Fujii, H., Journal of Alloys and Compounds. **330-332**, 526(2002)

[56] Sprunger, P.T. and Plummer, E.W. Chemical Physics Letters. **187**. 559(1991)

[57] Dahl, S. PhD Thesis, DTU, October 1999

[58] Yates. J.T. *Experimental Innovations in Surface Science*. Springer-Verlag 1998

[59] Fischer, A., Kostler, H., Schlapbach, L. Journal of the Less-common Metals. **172-174**. 808(1991)

[60] Delichere, P. and Bertolini, J.C., Surface and Interface Analysis. **34**. 116(2002)

[61] Dahl, S., Logadottir, A., Egebjerg, R., Larsen, J., Chorkendorff, I., Tørnqvist, E., and Nørskov, J.K..Physical Review Letters. **83**. 1814(1999)

[62] Krozer, A. and Kasemo, B. Surface Science Letters.**97**. L339(1980)

[63] He, J.W., Corneille, J.S., Goodman, D.W. Applied Surface Science. **72**. 335(1990)

[64] Wu, M-C., Corneille, J.S., Estrada, C.A., He, J-W, Goodman, D.W. Chemical Physics Letters. **182**. 472(1991)

[65] Huang, H.H., Jiang, X., Siew, H.L., Chin, W.S., Sim, W.S., Xu, G.Q., Surface Science. **436**. 167(1999)

[66] Arnold,A., Fahmi, A., Frie, W., Hammer, L., and Heinz, K. J. Phys.: Condensed Matter **11**, 1873(1999).

[67] Fukui, K., Aruga, T., Iwasawa, Y., Surface Science **281**, 241-252(1993).

[68] Gallagher, M.C., Fyfield, M.S., and Joyce, S.A. Physical Review B. **59**. 2346(1999)

[69] Wu, Y., Garfunkel, E., Madey, T.E. Surface Science. **365**. 337(1996)

[70] Vigeholm, B., Kjøller, J., Larsen, B., Pedersen, A.S. Journal of the Less-common Metals. **104**. 141(1984)

[71] Shao, H., Wang, Y., Xu, H., Li, X. Materials Science and Engineering B. **110**. 221(2004)

[72] Dehouche, Z., Goyette, J., Bose, T.K. and Schulz, R. International Journal of Hydrogen Energy. **28**. 983(2003)

[73] Hjort, P., Krozer, A., and Kasemo, B. Journal of Alloys and Compounds. **237**. 74(1996)

[74] Corneille, J.S., He, J-W., Goodman, D.W. Surface Science. **306**. 269(1994)

[75] Do, T., Splinter, S.J., Chen, C., McIntyre, N.S. Surface Science. **387**. 192(1997)

[76] Operation and Service Manual. Maxtek, Inc. 7th edition, June 2002

[77] Seah, M.P. and Dench, W.A. Surface and Interface Analysis. **1**, 2(1979)

[78] Somorjai, G. *Surface Chemistry and Catalysis*. John Wiley and Sons. 1994

[79] Pedersen A.S., Kjøller, J., Larsen, B., Vigeholm, B. International Journal of Hydrogen Energy. **Vol. 10, No. 12**. 851(1985)

[80] Pedersen, A.S., Vigeholm, B., Kjøller, J., Larsen, B. International Journal of Hydrogen Energy. **Vol.12, No.11**. 765(1987)

[81] Krozer, A., and Kasemo B. Journal of Physics: Condensed Matter. **1**. 1533(1989)

[82] Fernandez, J.F., Sanchez, C.R. Journal of Alloys and Compounds. **340**. 189(2002)

[83] Kratzer, P., Pehlke, E., Scheffler, M., Raschlke, M.B., and Höfer, U. Physical Review Letters. **81**, 5596(1998)

[84] Tessier, P., and Akiba, E. Journal of Alloys and Compounds. **293-295**. 400(1999)

[85] Oelerich, W., Klassen, T., Bormann, R. Advanced Engineering Materials. **3,7**.487(2001)

[86] Zeppelin, F., Reule, H. and Hirscher, M. Journal of Alloys and Compounds. **330-332**. 723(2002)

[87] Pelletier, J.F., Huot, J., Sutton, M., Schulz, R:, Sandy, A.R., Lurio, L.B. and Mochrie, S.G.J. Physical Review B. **63**. 52103(2001)

[88] Oelerich, W., Klassen, T., Bormann, R. Journal of Alloys and Compounds. **322**. L5(2001)

[89] Zhdanov, V.P., Krozer, A., and Kasemo, B. Physical Review B. **47**. 11044(1993)

[90] Vegge, T. Private communications

[91] Zeng, K., Klassen, T., Oelerich, W., Bormann, R. International Journal of Hydrogen Energy. **24**. 989(1999)

[92] Salomons, E. Journal of Phys. C: Solid State Physics. **21**. 5953(1988)

[93] Oskarsson, F., Stier, W., and Jonsson, H. Submitted. Physical Review B.

Included Papers

Paper I

Growth and Hydrogenation of ultra-thin Mg films on Mo(111)
Christopher W. Ostenfeld, Jon C. Davies, Tejs Vegge, and Ib Chorkendorff
Surface Science. **884**. 17(2005)

Paper II

Effect of Oxygen on the Hydrogenation Properties of Magnesium films
Christopher W. Ostenfeld and Ib Chorkendorff
In manuscript

Paper III

Hydrogenation Properties of Catalyzed and Non-catalyzed Magnesium Films
Christopher W. Ostenfeld and Ib Chorkendorff
In manuscript